Comments on Inorganic Chemistry

ADVENTURES OF QUANTUM CHEMISTRY IN THE REALM OF INORGANIC CHEMISTRY

CONSTANTINOS A. TSIPIS[a]

[a] Laboratory of Applied Quantum Chemistry, Thessaloniki, Greece

PLEASE SCROLL DOWN FOR ARTICLE

Taylor & Francis
Taylor & Francis Group

ADVENTURES OF QUANTUM CHEMISTRY IN THE REALM OF INORGANIC CHEMISTRY

CONSTANTINOS A. TSIPIS

Laboratory of Applied Quantum Chemistry, Faculty of Chemistry, Aristotle University of Thessaloniki, Thessaloniki, Greece

Recent improvements in the design of faster and more efficient algorithms have placed powerful computational quantum chemistry tools in the hands of all chemists. *ab initio* and density functional calculations are routinely performed by non-specialists in the field. These computational tools have nowadays become as useful to the bench chemist as spectrometers and vacuum lines. The impact of modern computational technology in the advancement of inorganic chemistry is outlined herein. Attempts have been made to present only the background information required to appreciate the general features of the computational quantum chemical techniques available and the types of chemical problems that can be reasonably solved in the growing field of quantum inorganic chemistry. It should be stressed that quantum chemical calculations assist experimental studies by accurately predicting chemical behavior. This is why a blend of theory and experiment must be effectively employed to solve a variety of difficult problems encountered in modern chemical research.

INTRODUCTION

The phenomenal increase in speed and computational power of computers has continued at an astonishing pace over the last decade. Chemistry, like many other disciplines, is being profoundly influenced by increased computing power. This has happened in part by enhancing many existing computational procedures, providing a new impetus to quantum

mechanical and molecular simulations at the atomic level of detail. Computational chemistry plays an increasing role in chemical research. With significant strides in computer hardware and software, computational chemistry has achieved full partnership with theory and experiment as a tool for understanding and predicting the behavior of a broad range of chemical, physical, and biological phenomena. With massively parallel computers capable of peak performance of several teraflops already on the scene and with the development of parallel software for efficient exploitation of these high-end computers, we can anticipate that computational chemistry will continue to change the scientific landscape in the 21st century. We are not far from the point where chemists can routinely design catalysts and other materials and predict biological activity or environmental fate from chemical structure.

Quantum chemistry, penetrating all chemistry, is the science that treats molecular behavior by one unified concept: the Schrödinger equation. Although there are specialists in the field, increasingly the computational quantum chemical techniques are being applied by chemists of many persuasions, who are experienced researchers knowing chemistry and now have computational tools available. Commercial programs incorporating the latest methods have become widely available and require little knowledge beyond the chemical formula to produce some results for a variety of properties. The ready availability and applicability of these programs provided a probe of structural, spectral, and reactivity characteristics frequently unavailable from experiment or, alternatively, facilitated interpretation of available experimental results. Noteworthy is the steadily increasing fraction of the articles listed in the current chemical journals that reference a computational chemistry software package.

Following the progress in the area of accurate quantum chemical treatment of systems containing transition metals in the last few years, a new, exciting field of inorganic chemistry—that of Quantum Inorganic Chemistry—has emerged. Computational methods for the analysis of transition metal containing molecular systems have undergone rapid progress in the recent past. Timely and important areas of computational chemistry concerning transition metal chemistry have been covered in recent special issues of *Chemical Reviews*[1] and *Coordination Chemistry Reviews*.[2] An earlier, comprehensive review of the theoretical approaches to the description of the electronic structure and chemical reactivity of transition metal compounds up to 1990 has also been reported in *Coordination Chemistry Reviews*.[3] Moreover, Koga and

Morokuma[4] reported an overview of theoretical studies of transition metal-catalyzed reactions, while Gordon and Cundari surveyed the recent advances in the effective core potential (ECP) studies of transition metal bonding, structure and reactivity.[5] Very recent reviews also cover some more specific topics of computational chemistry related to quantum chemical studies of intermediates and reaction pathways in selected metalloenzymes and catalytic synthetic systems[6] and the electronic structures of metal sites in proteins and models.[7]

The aim of the present article is to familiarize experimental chemists with the latest computational techniques and how these techniques can be applied to solve a wide range of real-world problems encountered in the realm of inorganic chemistry and particularly in transition metal chemistry. In addition, this article is meant to be a tutorial on the intelligent use of quantum chemical methods for the determination of molecular structure, reactivity and spectra of coordination and organometallic compounds.

APPLYING COMPUTATIONAL QUANTUM CHEMISTRY METHODS

The new comer to the field of computational quantum chemistry faces three main problems:

1. **Learning the language. The language of computational quantum chemistry is littered with acronyms. *What do these abbreviations stand for in terms of underlying assumptions and approximations?* If you want to use computational quantum chemistry methods, you need to decipher the acronyms.**
2. **Technical problems. *How does one actually run the program and what does one look for in the output*? This point related with both the hardware and software needs to be solved "on location." As computer programs evolve they become easier to use. In addition, modern programs often communicate with the user in terms of a graphical interface, and many methods became essentially "black box" procedures. This effectively means that we no longer have to be highly trained theoreticians to run even quite sophisticated calculations. Molecular modelling software lists can easily be found using the Internet.[8,9]**
3. **Quality assessment. *How good is the result of the calculation*? The accuracy of the various components of the computational methodology is of crucial importance to computational chemistry if we want theory and experiment to become partners in the solution of chemical problems.**

Because of the ease by which calculations can be performed this point has become the central theme in computational quantum chemistry. It is quite easy to run a series of calculations, which produce absolutely meaningless results, since the program cannot tell us whether the chosen method is valid for the problem we are studying. Therefore, quality assessment is an absolute requirement, but requires much more experience and insight than just running the program. Basic understanding of the theory behind the method and knowledge of the performance of the method for other systems is needed. In particular, when we want to make predictions, and not merely reproduce known results, we have to be able to judge the quality of the results obtained. Along this line a benchmark level of confidence in terms or robustness of structural and energetic results needs to be established, but this is by far the most difficult task in computational chemistry.

ELECTRONIC STRUCTURE CALCULATION METHODS

Electronic structure calculation methods are well-defined mathematical procedures aiming to solve the electronic Schrödinger's much-lauded wave equation in order to obtain the electronic wave function, $\Psi(\mathbf{r})$, which contains all the information for a particular state of a chemical system. A number of electronic structure calculation methods have been developed, each with advantages and disadvantages. These methods can be classified into the following three categories:

1. *ab initio* methods
2. Semi-empirical methods
3. Density Functional methods

In this section we will briefly outline the basic principles and terminology of the three classes of electronic structure calculation methods, starting at first principles, for the beginner in the field to feel comfortable in using these methodologies.

BASIC PRINCIPLES AND TERMINOLOGY OF AB INITIO METHODS

Ab initio methods are electronic structure calculation methods used to model the electron density in an atom or molecule with respect to the average electron density, without using any adjustable or empirically derived parameters in calculating the molecular energy. The reference

framework for the *ab initio* methods is the independent particle or molecular orbital (MO) model; the electrons are confined to certain regions of space. In practice, a number of approximations are made within the MO calculations that have a direct bearing on the reliability of the results obtained.

Born-Oppenheimer (BO) approximation: The first approximation in calculating molecular wave functions is the Born-Oppenheimer (BO) ''clamped nuclei'' approximation. It allows the motions of nuclei and electrons to be considered separately. In this way one obtains the time-independent non-relativistic electronic Schrödinger equation, which describes the motion of electrons in the field of fixed nuclei:

$$H|\Psi_e(\mathbf{r}; \mathbf{R})\rangle = E(\mathbf{R})|\Psi_e(\mathbf{r}; \mathbf{R})\rangle$$

The electronic Hamiltonian, H, of a molecular system with N electrons and M nuclei, contains one- and two-electron terms consisting of all of the kinetic and potential energy terms that act upon the electrons:

$$H = -\sum_{i=1}^{N} \frac{1}{2}\nabla_i^2 - \sum_{i=1}^{N}\sum_{A=1}^{M} \frac{Z_A}{r_{iA}} + \sum_{i=1}^{N}\sum_{j=1}^{N} \frac{1}{r_{ij}}$$

In the framework of the BO approximation the electronic wave function $\Psi_e(\mathbf{r}; \mathbf{R})$ depends parametrically on the nuclear coordinates $\mathbf{R}$. By parametric dependence we mean that, for different arrangements of the nuclei, $\Psi_e(\mathbf{r}; \mathbf{R})$ is a different function of the electronic coordinates. In the BO approximation, the energy $E(\mathbf{R})$ of the electronic Schrödinger equation provides a potential for the motion of the nuclei. In other words, the electrons are dragged along the nuclei, and the dressed nuclei (atoms in molecules) move in the field of the electronic distribution. These electronic energies' dependence on the positions of the nuclei causes them to be referred to as potential energy surfaces (PES), which will be discussed latter on. Most computational chemical studies involve characterizing key features of the PES or integrating the trajectories on this surface.

Hartree-Fock (HF) approximation: In the HF approximation the inter-electronic repulsion term,

$$\sum_{i=1}^{N}\sum_{j=1}^{N} \frac{1}{r_{ij}}$$

of the electronic Hamiltonian is replaced with an effective potential $V(r)$, which represents the potential one electron "feels" when moving independently of the others in the field created by the fixed nuclei and the mean-fields of the other electrons. This substitution allows us to reduce the N-particle problem to a set of one-particle eigenvalue problems,

$$F(\mathbf{r_i})\varphi_i(\mathbf{r_i}) = \varepsilon_i \varphi_i(\mathbf{r_i})$$

and is the basis of molecular orbital theory. These nonlinear equations are referred to as Hartree-Fock or SCF (Self Consistent Field) equations. The term orbital (atomic, AO or molecular, MO) was created for the one-electron wave function $\varphi_i(\mathbf{r_i})$. An MO is an eigenfuction of an effective one-particle Hamiltonian, the so-called Hartree-Fock operator, F and the electron in the MO is considered to have an orbital energy of ε_i.

Basis set approximation: In the basis set approximation, introduced by Roothaan in 1951, each MO $\varphi_i(\mathbf{r_i})$ should be expanded algebraically as a finite set of basis functions χ_μ, which are normally centered on the atoms in the molecule. This gives,

$$\varphi_i(\mathbf{r}_i) = \sum_{\mu=1}^{N} c_{i\mu}\chi_\mu$$

The basis functions collectively are the *basis set*. The coefficients for a given MO can be thought as arrays that, when squared and added together, will produce a density matrix **P** with elements given by:

$$P_{\mu v} = 2 \sum_{i=1}^{occ} c_{i\mu}c_{iv}$$

Here the sum runs over the occupied orbitals of the system. The density matrix and its associated orbital basis set are all that is needed to compute electronic properties of the molecular system.

Introducing the basis set approximation into the SCF equations the eigenvalue problem is converted into a matrix problem,

$$\mathbf{FC} = \mathbf{SC}\varepsilon,$$

which can be solved iteratively. From a practical standpoint, these simplifications allow an initial guess at the electron configuration of the chemical system to produce a guess at the effective potential, which can be used as an improvement to the guess of the orbitals, etc. Once the orbitals and the potential no longer change, the iterative calculation is complete; it is

said to be *self-consistent*, which is why the HF approximation as practiced today is generally synonymous with SCF in the literature. In the HF approximation the energy of the molecular system is computed variationally with respect to the coefficients $c_{i\mu}$ and can be written as:

$$E_{\text{HF}} = \sum_{\mu\nu} P_{\mu\nu} H_{\mu\nu} + \sum_{\mu\nu\lambda\sigma} P_{\mu\nu} P_{\lambda\sigma} (J_{\mu\nu\lambda\sigma} - K_{\mu\nu\lambda\sigma}) + V_{\textit{nucl}}$$

Here the Hamiltonian matrix elements $H_{\mu\nu}$ are the terms referring to the kinetic energy and the potential energy of attraction between the electrons and the nuclei. The Coulomb integrals $J_{\mu\nu\sigma\lambda}$ are the terms referring to the potential energy of repulsion between pairs of electrons, while the Exchange integrals $K_{\mu\nu\sigma\lambda}$ are the terms arising from the antisymmetry of the wave function with respect to exchange of any two electrons. Finally, the term V_{nuc} is the potential energy from the repulsion of pairs of nuclei.

The basis function χ_{μ} can be thought of as atomic orbitals (*s, p, d,* etc.) from the rigorous solution of Schrödinger's equation for the hydrogen atom. For many-electron atoms, we don't know the actual mathematical functions for the atomic orbitals, so substitutes are used, usually either Slater-type orbitals (STO) or Gaussian-type orbitals (GTO). We don't concern ourselves with the exact form of STOs and GTOs. Suffice it to say that they are chosen to behave mathematically like the actual atomics orbitals of *s*-, *p*-, *d*-, *f*-type, etc. The use of GTOs is now common. This is because it is very difficult to evaluate the necessary integrals over STOs when the orbitals in the integrand are centered on three or four different atoms. In practice the basis functions are often fixed linear combinations of GTOs whose exponents have been judiciously chosen by minimizing atomic energies, matching STOs, or by reproducing experimentally known molecular properties.

There is a bewildering number of basis sets tabulated and tested in the literature for almost every element of the periodic table, and still more are developed each year.[10,11] They are symbolized by acronyms, which are also used as keywords in the computer codes that perform quantum chemical calculations. Basis sets could be classified as follows:

1. *Minimal basis sets*
2. *Split valence basis sets*
3. *Extended basis sets*

Important additions to basis sets are *polarization* and *diffuse* basis functions. *Polarization* functions[12–14] are functions added in the basis

set to distort the shape of the orbitals (in principle the atomic orbitals) due to their polarization introduced by the other nuclei in the molecular system. The distortion of an atomic orbital is accomplished by adding in basis functions of higher angular momentum quantum number. *Diffuse* functions are necessary to be added in the case of investigating *excited states* and *anionic species* because in these cases the electronic density is more spread out over the molecule. To model this correctly we have to use basis functions which themselves are more spread out. These functions are GTOs with small exponents.

For transition metal complexes, because of the large number of basis functions that must be included to model the non-valence electrons in the metals, particularly those of the second and third row, the inner shell electrons are replaced by a model potential called *effective core potential* (ECP).[5,15,16] The ECPs not only reduce the computational demands of calculations on transition metal compounds but they also allow the inclusion of relativistic effects for the heavier second- and third-row transition metals, in a straightforward manner. The relativistic effective core potentials (RECPs) are generated from the relativistic HF atomic core. The ECP schemes of LANL2DZ and SDD have performed extremely well with respect to the calculation of the equilibrium geometries of transition metal complexes and organometallics. In addition, extra basis sets of at least the 6-31G(d,p) quality must be used for the non–metal and hydrogen atoms. Generally, the larger the basis set the more accurate the calculation (within limits) and the more computer time that is required. A few commonly used basis sets are listed in Table 1.

Correlated or Post-HF Models

Because of the central field imposed by the HF potential $V(r)$, each electron is not explicitly aware of the others' presence. It is usually said that the HF models neglect *electron correlation*, because there is a finite probability that two electrons will occupy the same point in space. Electron correlation, the energy of which is defined as the difference between the exact energy, E_{exact} of a system and the HF limit energy, E_{HF}, which is obtained using an essentially complete basis set, is neglected in the HF approach. Correlation energy will always be negative because HF energy is an upper bound to the exact energy E_{exact}.

$$E_{correlation} = E_{exact} - E_{HF} < 0$$

Table 1. Acronyms of the most commonly used basis sets

Basis set	Characteristics
STO-3G	A minimal basis set using three GTO to approximate each STO.
3-21G	A split valence basis set. Inner shell basis functions made of three GTOs. Valence orbitals are split into 2 and 1 GTOs.
6-31G	A split valence basis set. Inner shell basis functions made of six GTOs. Valence orbitals are split into 3 and 1 GTOs.
6-31G(d) or 6-31G*	The 6-31G basis set with the addition of six d-type polarization functions to non-hydrogen atoms.
6-31G(d,p) or 6-31G**	The 6-31G(d) basis set with the addition of p-type polarization functions to non-hydrogen atoms.
6-31G + (d,p) or 6-31 + G**	The 6-31G(d,p) basis set with the addition of s- and p-type diffuse functions to the atoms of first and second rows.
6-31G + + (d,p) or 6-31 + + G**	The 6-31G(d,p) basis set with the addition of a set of s- and p-type diffuse functions to the atoms of first and second rows and a set of s-type functions to hydrogen.
6-311G	A split valence basis set. Inner shell basis functions made of six GTOs. Valence orbitals are triply split into 3, 1, and 1 GTOs.
D95	Dunning/Huzinaga full double zeta.
CEP-121G	Stevens/Basch/Krauss ECP triple-split basis.
LanL2DZ	D95V on first row and Los Alamos ECP plus DZ on Na–Bi.
SDD	D95V up to Ar and Stuttgart/Dresden ECPs on the remainder of the periodic table.
cc-pVDZ, cc-pVTZ, cc-pVQZ, cc-pV5Z, cc-pV6Z	Dunning's correlation consistent basis sets (double, triple, quadruple, quintuple-zeta and sextuple-zeta, respectively).

Higher levels of theory are necessary to resolve this issue by recovering the correlation energy. Most of the standard high-level techniques in quantum chemistry utilize the HF approximation as a starting point and then attempt to correlate electrons by more rigorous computational methods. A large number of such methods have been used to improve the HF method, which can be classified into two classes:

1. *Variational methods*
2. *Perturbational methods*

Variational methods: A common method for incorporating correlation into HF calculations is to construct a modified wavefunction using the unoccupied (vitual) orbitals of the "reference" HF wavefunction. In this approach, which is termed Configuration Interaction (CI), method, contributions from excited configurations (single excited, Ψ_i^a, double excited, Ψ_{ij}^{ab}, etc.), in which electrons are promoted from the occupied (filled) $i, j,\ldots$, MOs to the "virtual" $a, b,\ldots$, MOs, are mixed variationally with the ground state wavefunction Ψ_0 to give the following expression:

$$\Psi = c_0\Psi_0 + \sum_{ia} c_i^a \Psi_i^a + \sum_{ij} c_{ij}^{ab}\Psi_{ij}^{ab} + \cdots$$

If the set of the determinantal wave functions included in the CI calculation is complete, it is a full CI calculation (FCI) and is both variational and size-consistent. However, an FCI calculation is extremely expensive and impractical for all but the tiniest of molecular systems. Therefore, the CI expansion should be limited in one way or another. More realistically, the set of determinantal wave functions could include only the double (D) excited configurations (denoted CID) or the single (S) and double (D) excited configurations (denoted CISD). It is also typical to augment the CISD calculations with triple (T) and/or quadruple (Q) excitations, with the most popular variant being the quadratic configuration interaction denoted as QCISD. In general, CI is not the practical method of choice for calculation of correlation energy, because FCI is not possible, convergence of the CI expansion is slow, and the integral transformation time-consuming. However, an advantage of the CI method is that it is variational, so the calculated energy is always greater than the exact energy.

Other approaches aim to optimize not only the mixing coefficients of the various configurations, but also the coefficients of the basis functions in the molecular orbitals. The latter are frozen at the HF values in the CI methods described above. This more complex approach is called multi-configuration self-consistent field (MCSCF). It can give quite good results with a modest number of configurations. The CASSCF—Complete Active Space Self-Consistent Field—method is an example of this approach. Using CASSCF, the references are selected by choosig an "active space" of several chemically important orbitals and performing

a FCI in the span of the active space. The MCSCF method requires considerable care in the selection of the basis set and especially the active space, and should not be considered for routine use. MCSCF methods are essential for the study of processes in which transitions between potential energy surfaces occur, such as in photochemical reactions.[10,17–22]

Perturbational methods: There are two important perturbative post-HF methods: many-body perturbation theory (MBPT) and coupled cluster (CC).

In perturbation theory we define a perturbed Hamiltonian $H(\lambda)$:

$$H(\lambda) = F_0 + \lambda[H(\lambda) - F_0]$$

where F_0 is the HF operator with an appropriate eigenfunction Ψ_0 if $\lambda = 0$, and the exact (FCI) eigenfunction Ψ obtained if $\lambda = 1$, while the energy $E(\lambda)$ of the perturbed system is expanded in MacLaurin series:

$$E(\lambda) = E_0 + \lambda E_1 + \lambda^2 E_2 + \lambda^3 E_3 + \cdots$$

including corrections of first, E_1 second, E_2, third, E_3 order, etc.

A particularly successful application to molecules and the correlation problem goes back to Møller and Plesset in 1933.[23] This is now the MPn methods. The first important correction is the second order term E_2 and this leads to MP2. MP2 is relatively economic to evaluate and gives a reasonable proportion of the correlation energy. Higher order terms become more and more expensive. MP3 is commonly used, but does not seem to give much improvement over MP2. An enormous practical advantage is that MP2 is fast (of the same order of magnitude as SCF), while it is rather reliable in its behavior, and size consistent. A disadvantage is that it is not variational, so the estimate of the correlation energy can be too large. In practice MP2 must be used with a reasonable basis set (6–31 G* or better).

In the coupled cluster method,[22,24–26] which is by far the most popular high-level *ab initio* quantum chemical method today, the electron correlation effects are treated in a different way. The CC method allows to mix in the higher configurations by constructing an exponential operator e^T that acts on the HF ground state to produce configurations from only a certain class of excitations.

$$\Psi = e^T \Psi_0$$

T is an excitation operator: $T = T_1 + T_2 + \cdots + T_n$.

The excitations are usually limited to single, double and triple substi-tutions. Since carrying out the exponential as a sum will generate many new configurations that are sums of products of the configurations, this technique is known as coupled cluster singles, and triples (CCSDT) theory. Triple excitations can also be included in an approximate but less time-consuming way, leading to the CCSD(T) method. Armed with this powerful technique, something like 97% of the correlation energy can be extracted from just the first three terms in T. Unfortunately, these most sophisticated correlation methods at the present time are extremely costly in terms of time and resources.

BASIC PRINCIPLES AND TERMINOLOGY OF SEMI-EMPIRICAL METHODS

The common *ab initio* molecular orbital techniques can only be applied with difficulty to transition metal systems. They are limited in their prac-tical applicability because of their heavy demands of CPU-time and storage space on disk or in the computer memory. At the HF level the problem is seen to be in the large number of two-electron integrals that need to be evaluated. Without special tricks this is proportional to the fourth power of the number of basis functions. The first strategy used to reduce computational effect is to consider only valence electrons in the quantum mechanical treatment. The core electrons are accounted for in a core-core repulsion function, together with the nuclear repulsion energy. The next step is to replace many of the remaining integrals by parameters, which can either have fixed values, or depend on the distance between the atoms on which the basis functions are located. At this stage empirical parameters can be introduced, which can be derived from measured properties of atoms or diatomic molecules. In the modern semi-empirical methods the parameter are however mostly devoid of this physical significance: they are just optimized to give the best fit of the com-puted molecular properties to experimental data. Different semi-empirical methods differ in the details of the approximations (e.g. the core-core repulsion functions) and in particular in the values of the parameters.

Nowadays, semiempirical MO-theory is usually taken to mean the modern variants of neglect of differential diatomic overlap (NDDO)[27] theory. New versions of the NDDO methods have recently been developed that include *d*-orbitals for second-row and heavier elements: Modified Neglect of Diatomic Overlap (MNDO/d),[28] extended Austin

Model 1 (AM1),[29] Parametric Method (PM3),[30] and PM3(tm).[31] Commercial programs like MOPAC embody a suite of methods from which a knowledgeable modeller can make an optimum selection. Recently, a slightly extended and reparameterized version of PM3 termed PM5 has been made available in MOPAC.

BASIC PRINCIPLES AND TERMINOLOGY OF DENSITY FUNCTIONAL METHODS

Given the computational problems associated with the application of *ab initio* molecular orbital-based methods to problems of structure and reactivity in coordination and organometallic compounds, most theoretical studies in this area employ density functional theory (DFT) methods.[33–35] In a nutshell, DFT is based on the fact that all molecular electronic properties can be calculated if the electron density $\rho(\mathbf{r})$ is known. Thus, the molecular properties are functionals of $\rho(\mathbf{r})$ because the electron density itself is a function of the spatial coordinates $\mathbf{r}$. In the framework of DFT the ground state electronic energy of an N electron system can be expressed by:

$$E_{\mathrm{DFT}} = \sum_{\mu\nu} P_{\mu\nu} H_{\mu\nu} + \sum_{\mu\nu\lambda\sigma} P_{\mu\nu} P_{\lambda\sigma} J_{\mu\nu\lambda\sigma} + E_{\mathrm{X}}(\rho) + E_{\mathrm{C}}(\rho) + V_{\mathrm{nuc}}$$

where $E_{\mathrm{X}}(\rho)$ and $E_{\mathrm{C}}(\rho)$ are two empirically derived functions that replace the exchange matrix and referred to as the exchange and correlation functionals, respectively. A starting point based upon a SCF procedure is developed which ultimately determines the ground state charge and spin densities, through solution of the single particle Kohn-Sham equations.[36] DFT provided a sound basis for the development of computational strategies for obtaining information about the structure, energetics, and properties of molecules at much lower costs than traditional *ab initio* wave function techniques. An excellent publication by Koch and Holthausen in 2000, entitled *Chemist's Guide to Density Functional Theory*,[33] offers an overview of the performance of DFT in the computation of a variety of molecular properties, thus providing a guide for the practicing, not necessarily quantum, chemists. Moreover, a recent survey of chemically relevant concepts and principles extracted from DFT, the so-called conceptual DFT by Geerlings *et al.* is very informative.[37]

Despite its simple origins, DFT works very well in most cases. For about the same cost of doing a HF calculation, DFT includes a

significant fraction of the electron correlation. Note that DFT is *not* a HF method, nor is it (strictly speaking) a post-Hartree-Fock method! The wave function is constructed in a different way and the resulting orbitals are often referred to as ''Kohn-Sham'' orbitals. The KS orbitals appear to be as robust as HF orbitals for qualitative interpretation and rationalization of molecular properties. The chief difference between the SCF and KS-DFT approaches lies in the exchange-correlation (XC) density functionals. If the exact form for the XC functionals were known, the KS-DFT approach would give the exact energy. There are, however, a number of approximate functionals available, which can be classified as:

- **Functionals based on the local density approximation (LDA).[38] For these functionals the energy depends only on the charge density $\rho(\mathbf{r})$.**
- **Functionals based on the generalized gradient approximation (GGA).[39–41] These functionals use not only the value of the electron density $\rho(\mathbf{r})$, but also its gradient $\nabla\rho(\mathbf{r})$.**
- **Meta-GGA functionals. For these functionals the energies depend also on the Laplacian of the density $\nabla^2\rho(\mathbf{r})$ and/or the orbital kinetic energy.**
- **Hybrid density functionals combining GGA functionals with a parameterized proportion of the exchange energy calculated by HF theory.[42]**

Some of the most popular functionals you may come across are:

BP86 – developed by Becke and Perdew in 1986.
B3PW91 – a three-parameter functional expression including the PW91 correlation functional.
BLYP – developed by Becke, Lee, Yang and Parr.
B3LYP – a modification of BLYP in which a three-parameter functional developed by Axel Becke is used.
MPW1K – modified Perdew-wang 1-parameter model for kinetics developed by Donald G. Truhlar *et al.*[43]

The choice of the functional is the only limitation of the DFT method. At the present time, there is no systematic way of choosing the functional and the most popular ones in the literature have been derived by careful comparison with experiment. It should be emphasized

that great care has to be exercised in choosing the DFT functional to calculate properly spin states in transition metal complexes.
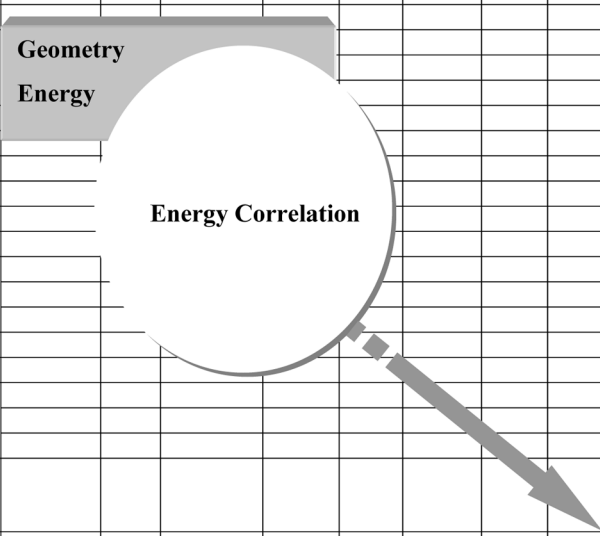
Quality and Reliability of Quantum Chemical Results

The combination of a quantum chemical computational method and a basis set defines a ''model chemistry.'' A model chemistry should be uniformly applicable and tested on as many systems as possible to asses its performance. The strategic use of model chemistries that can be practically applied for inorganic molecules with present-day hardware and software, based on the computational method and the basis set, is compiled in Table 2.

The various correlation methods are displayed vertically in order of increasing sophistication from top to bottom. Basis sets are displayed

Table 2. Basis set versus quality of theory in *ab initio* calculations, illustrating their strategic use in transition metal chemistry

Method	Basis Set								
	Minimal	DZ	6-31G**	DZP	TZP	PVTZ	QZP	....	Complete Basis
HF									
DFT									
MP2									
CISD									
MP3									
CCD									
CCSD									
MP4									
MCSCF									
QCISD(T)									
CCSD(T)									
MR-CI									
.									
.									
.									
FULL CI									TRUE

horizontally, becoming more flexible from left to right. At the bottom of the table, full configuration interaction (FCI) represents complete solution within the finite space defined by the basis set. At the far right, the results of applying a complete basis set are found (in principle but not in practice). At the bottom right, application of a complete basis set with full CI corresponds to full solution of the time-independent nonrelativistic Schrödinger equation. Each empty box represents a well-defined size-consistent theoretical model. Clearly, we may test each level to find how far we have to proceed from the top left to the bottom right for acceptable agreement between theory and experiment. In practice, full models usually have to make some compromises to achieve a wide range of applicability. If the prediction of energies is most important, a common practice is to carry out a geometry optimization at some lower level of theory (model-1) and then make a final, more expensive, computation at a higher level (model-2). A useful notation for this type of composite model is model-2//model-1.

The reliability of chemical properties calculated with the most rigorous quantum chemical computational methods listed in order of difficulty:

- **Molecular structure ($\pm 1\%$)**
- **Reaction Enthalpies ($\pm 1\,\text{kcal/mol}$)**
- **Reaction Free Energies ($\pm 2\,\text{kcal/mol}$)**
- **Vibrational Frequencies ($\pm 5\%$)**

CAPABILITIES OF COMPUTATIONAL QUANTUM CHEMISTRY METHODS

Using computational quantum chemical methods, the following operations may be performed:

- **Geometry optimization**
- **Single-point energy calculation**
- **Predicting barriers and reaction paths**
- **Calculation of wave functions and detailed descriptions of molecular orbitals**
- **Calculation of atomic charges, dipole moments, multipole moments, electrostatic potentials, polarizabilities, etc.**
- **Calculation of vibrational frequencies, IR and Raman intensities**

- Calculation of NMR chemical shifts
- Calculation of ionization energies and electron affinities
- Time-dependent calculations
- Inclusion of the electrostatic effects on solvation

Geometry Optimization

Geometry optimization is the computational procedure of finding the equilibrium geometry of a molecule, e.g. the geometry of the lowest possible energy. The procedure calculates the wave function and energy at a starting geometry, which can be usually input in the form of a Z-matrix or in Cartesian coordinates and then proceeds to move to a new geometry, which will give a lower energy. This is then repeated until the lowest energy geometry close to the starting point is obtained. The optimization procedure calculates the forces on the atoms by evaluating the gradient of the energy with respect to atomic coordinates analytically or in some cases numerically. The mathematical and computational machinery for structure optimization is based on various algorithms, the complexity of which depends on the desired accuracy of the electronic level. Sophisticated algorithms (such as those based on the steepest descent, Newton-Raphson, simplex, Fletcher-Powell and combined methods) are used to select a new geometry at each step, which gives rapid convergence to the geometry with the lowest energy.

It is important to recognize that the optimization procedure will not necessarily find the geometry of lowest energy, the so-called global minimum (point **a**) in the potential energy surface (Figure 1).

It may find a local minimum (point **e**). It is the staring geometry, which determines which of the minima would be obtained by optimization. Thus, if the starting geometry was that at point **b** of the PES the global minimum is obtained, while if it was at point **d** the local minimum is obtained. Besides the location of minima (global or local) on the PES the optimization process could also locate some other stationary points corresponding to transition states or other maxima (saddle points). We can sort out the types of stationary points by carrying out frequency calculations. With the development of common efficient analytical energy gradients, $g_i = \partial V(x)/\partial x_i$ and second derivatives, $G_{ij} = \partial^2 V(x)/\partial x_i \partial x_j$ (Hessian matrix) methods, complete optimization of geometric parameters for minima and saddle points has become more common.

If the geometry obtained from an optimization run is a local or indeed the global minimum, all the frequencies (e.g. the eigenvalues of
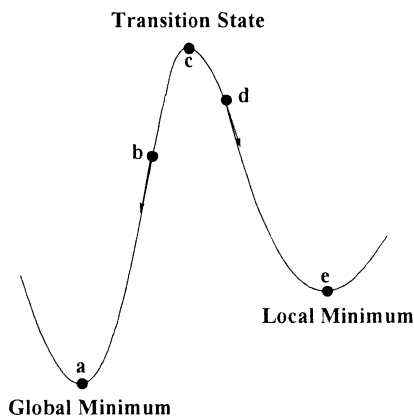
Figure 1. Part of a potential energy surface (PES) in a 2D space.

the Hessian matrix) will be real and positive. If we have a transition state (TS) or any stationary point other than a minimum, some of the frequencies will be complex (negative eigenvalues of the Hessian) and are often called "imaginary frequencies." Transition structures (point **c**) usually connecting two stationary structures (points **a** and **e**) will have one imaginary frequency. In summary, the nature of stationary points on the PES can be characterized by the number of imaginary frequencies (NImag): NImag = 0 for a minima; NImag = 1 for a TS (first-order saddle point); NImag = n for a "maximum" (n-order saddle point). Note that frequency calculations should only be carried out at the geometry obtained from an optimization run and with the same basis set and method.

Currently, the most common geometry optimizations for transition metal coordination compounds and organometallics are performed at the HF, MP2, and DFT levels of theory. In particular, the new generation of gradient-corrected DFT methods such as the B3LYP, BP86 and BW91 variants are efficient and accurate computational methods for these studies. The single-reference HF and MP2 methods could not yield reliable results for the geometry optimization of first-row transition metal compounds, since the compactness of the $3d$ orbitals leads to the presence of strong near-degeneracy effects, thus leading to multi-reference character in the state of interest. It is always a good idea to do a geometry optimization with a small basis set and a poor method before we move to the basis set and method of choice for the molecular system of interest

in relation to the molecular size and the computational resources available. An acceptable ''chemically accurate'' calculation of the geometrical parameters should give for the bond lengths and bond angles values within 0.01–0.02 Å and 1–2° of experiment, respectively. Notice that the only way to obtain molecular structures that converge toward the correct result is to use increasingly larger basis sets and more complete treatment of electron correlation. As a general rule increasing the electron correlation increases bond length (and by consequence reduce bond angles), while basis set enlargement exhibits the opposite behavior.

Single Point Energy Calculations

This procedure simply calculates the energy, wave function and other requested properties at a single fixed geometry. It is frequently carried out after a geometry optimization, but with a larger basis set or a more superior method than is possible with the basis set and method used to optimize the geometry. Thus for a very large system, such as transition metal compounds, the geometry may be optimized at B3LYP level with a small basis set, but energy is calculated with the MP2, MCSCF, MCPF, or CCSD(T) methods and a larger basis set. In general terms DFT methods give a much better and more reliable description of the geometries and relative energies than HF and MP2 methods except for some weak bonding interactions. Hydrogen-bonding and proton-transfer reactions are generally not treated well by DFT.[44,45] It should be stressed that DFT methods (such as B3LYP and B3P86) became the dominant computational tool for treating the transition metal compounds. Only CC methods, which are very costly, would appear to equal or exceed the accuracy of the best DFT methods.

Predicting Barriers and Reaction Paths

An important use of electronic structure calculations is the determination of barrier heights for chemical reactions, because such barriers play a crucial role in determining the rates of the reactions. The essential features of a chemical reaction mechanism are contained in the minimum energy path(s)–the path(s) of steepest descent connecting reactants and products via transition states. A schematic of such a minimum energy path (also referred to as an intrinsic reaction coordinate, IRC) is shown in Figure 2. The reaction coordinate represents a composite change in all geometric parameters (angles and bond lengths) as the reaction proceeds. Short
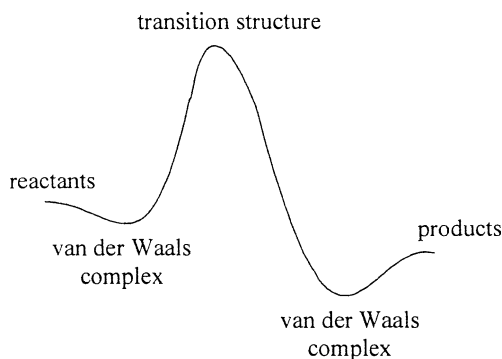
Figure 2. Hypothetical reaction coordinate.

of determining an entire reaction coordinate, there are a number of structures and their energies that are important to defining a reaction mechanism. For the simplest single step reaction, there would be five of these structures shown in Figure 2.

1. **The reactants**
2. **The precursor van der Waals complex between the reactants**
3. **The transition structure**
4. **The precursor van der Waals complex between the products**
5. **The products**

Reactants and products correspond to energy minima, whereas transition states linking products to reactants usually correspond to first-order saddle points on the energy surface (although unusual symmetries can produce higher order transition states, including those of the "monkey-saddle" type). Thus, the location of stationary points (particularly minima and saddle points) on potential energy surfaces represents an important and challenging problem in computational chemistry.

The PES's topology governs how much of a hill or barrier there is to each elementary reaction step and whether the process is thermodynamically favorable. This is referred to as the *energetic reaction profile.* The recent survey of some practical methods in use to explore PESs for chemical reactions by Schlegel is very informative.[46]

As a general rule of thumb, transition structures are more difficult to describe than equillibrium geometries. The location of saddle points on the PES is more difficult than finding local minima. However, a number

of clever algorithms have been developed in the past decade. Generally, if a program is given a molecular structure and told to find a TS, it will first compute the Hessian matrix. The nuclei are then moved in a manner that increases the energy in directions corresponding to negative eigenvalues of the Hessian and decreases energy where there are positive eigenvalues. This is a quasi-Newton technique, which implicitly assumes that the PES has a quadratic shape. Thus the optimization will only be able to make the correct geometry if the starting geometry is sufficiently close to the TS geometry to make this a valid assumption. One excellent technique is to start with a geometry with bond lengths of the bonds being formed or broken intermediate to their bonding and van der Walls lengths.

Since TS structure calculations are so sensitive to the starting geometry, a number of techniques for finding reasonable starting geometries have been proposed. One very useful technique is to start from the reactant and product structures, which are more easily obtained than TS structures. In this category belong the quadratic synchronous transit methods (OST2 and QST3). In QST2 the software package will require the user to provide as input the structures of reactants and products, while in QST3 a possible transition structure is also required. The QST techniques fail for multi-step reactions, but can be used individually for each step.

TS structures can also be obtained by following the reaction path from the equillibrium geometry to the TS. This technique is known as eigenvalue-following (EF) because the user specifies which vibrational mode should lead to a reaction given sufficient kinetic energy.

Another way to reliably find a TS is based on the scan of the PES through a series of calculations representing a grid of points on the PES. The saddle point can then be found by inspection, or more accurately by using mathematical techniques to interpolate between the grid points. However, this is a very time–consuming method and is only used when the research requires obtaining a PES for reasons other than finding the TS.

Nonetheless, the aforementioned saddle point searches sometimes fail to converge, or they converge to critical points that are minima; thereby more robust algorithms are still needed.
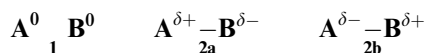
Once the TS has been obtained, it may be useful to consider the exact path that lead back to the reactants and forward to the products using the IRC method. The IRC provides a nice rubric for thinking about the course of a chemical reaction and, combined with variational state theory, allows the calculation of the reaction rates as well.

Molecular Orbitals and Electron Density

Molecular orbitals (MOs) are not real physical quantities. Orbitals are a mathematical convenience that help us think about bonding and reactivity, but they are not physical observables. Many quantum chemistry programs have graphical interfaces that allow the schematic representation of MOs. Among the various MOs of a molecule, the Highest Occupied (HOMO) and Lowest Unoccupied (LUMO) are of particular interest for the qualitative prediction of the chemical reactivity and selectivity. Most important is the electron density related to the probability that an electron will occupy a precise point of space, which is a measurable real physical quantity. Notice that any property is a result of the electron density. A surface of constant electron density (isosurface) serves several functions depending on the value of the density at the surface. Surfaces of very high electron density identify atomic positions (the basis of the X-ray diffraction experiment). Surfaces corresponding to somewhat lower electron density can be used to "assign" bonds in molecules where there may be more than one reasonable alternative. Perhaps the most important use of electron density surfaces is to depict overall molecular size and shape, the same information that is provided by a space-filling model. For instance, the 0.001 electron density isosurface is often used to show the spatial extent of a molecule. It surrounds that part of space that has the largest probability of containing the electrons. Moreover, electron density isosurfaces indicate the preferred positions for the nucleophilic and electrophilic attack of the molecule of interest.

Atomic Charges Dipole Moments and Multipole Moments

One of the most generally used concepts in chemistry is the atomic charge, which has the following intuitive meaning: when two noninteracting atoms $\mathbf{A}$ and $\mathbf{B}(\mathbf{1})$ form a chemical bond ($\mathbf{2}$), the atomic charge of $\mathbf{A}$ resulting from the formation of the chemical bond is the amount of electron density gained from ($\mathbf{2a}$) or lost to ($\mathbf{2b}$) atom $\mathbf{B}$:

$$\mathbf{A}^0 \; \mathbf{B}^0 \qquad \mathbf{A}^{\delta+}\!\!-\!\mathbf{B}^{\delta-} \qquad \mathbf{A}^{\delta-}\!\!-\!\mathbf{B}^{\delta+}$$
$$\quad\;\;{}_{\mathbf{1}} \qquad\qquad\quad {}_{\mathbf{2a}} \qquad\qquad\quad {}_{\mathbf{2b}}$$

Several methods for the quantification of the atomic charges have been developed over the years trying to solve the problem of how one can partition the electron density, which does not by definition belong

to any atom, over the different atoms. Different ways of partitioning lead to different numbers for the atomic charges and therefore possibly to different ways of interpreting the nature of the chemical bond.

The oldest and also the best-known definition of the atomic charge is the Mulliken population analysis.[47] This method uses the basis functions χ_μ, in terms of which the molecular wave function $\varphi_i(\mathbf{r})$ is expressed. The total number of electrons N of the molecule is then given by

$$N = n_i \sum_{i=1}^{occ} \langle i | i \rangle = \sum_{A,B} \sum_{\mu \in A} \sum_{v \in B} \sum_{i=1}^{occ} n_i c_{\mu i} c_{vi} \langle \mu | v \rangle$$

$$= \sum_{A,B} \sum_{\mu \in A} \sum_{v \in B} \sum_{i=1}^{occ} n_i P_{\mu v} S_{\mu v}$$

with orbital occupations n_i. The diagonal elements of $P_{\mu\mu}S_{\mu\mu}$ represent the net Mulliken population that basis functions acquire in the molecule. The gross Mulliken population Q_μ for all basis functions is obtained by assigning half of each total overlap population $(P_{\mu v}S_{\mu v} + P_{v\mu}S_{v\mu})$ to this basis function:

$$Q_\mu = P_{\mu\mu}S_{\mu\mu} + \sum_{v \neq \mu} \frac{1}{2}(P_{\mu v}S_{\mu v} + P_{v\mu}S_{v\mu})$$

The Mulliken charge of atom A is obtained by summing up the gross population Q_μ for all basis functions χ_μ centered on that atom and substracting them from the corresponding charge Z_A, as shown in

$$Q_A^{Mulliken} = Z_A - \sum_{\mu \in A} Q_\mu$$

The Mulliken charges based on the wave function representation as a linear combination of basis functions are heavily basis set dependent and in principle do not converge with increasing basis set size. Moreover the half-to-half partitioning of the Mulliken population analysis yields totally unphysical charges. Attempts to circumvent these problems lead to the development of a population scheme, the natural population analysis (NPA).[48] The NPA is performed on the optimized polyatomic wave function employing explicitly orthogonal (natural) atomic orbitals, and thus solves the overlap problem. Natural bond orbital analysis (NBO) transforms the input basis set to various localized basis sets (natural atomic orbitals, NAOs, hybrid orbitals, NHOs, bond orbitals, NBOs,

and localized molecular orbitals, NLMOs):

Input basis set $\rightarrow$ NAOs $\rightarrow$ NHOs $\rightarrow$ NBOs $\rightarrow$ NLMOs

The localized sets may be subsequently transformed to delocalized natural orbitals (NOs) or canonical molecular orbitals (CMOs). Each step of the above sequence involves an orthonormal set that spans the full space of the input basis set and can be used to give an exact representation of the calculated wave function and the expectation values of selected properties of the system.

More realistic atomic charges are obtained by population analysis schemes that are based on the electron density. In this category belong the methods developed by Bader,[49] Hirshfeld,[50] Politzer and coworkers,[51] Van Alsenoy and coworkers[52] and the Vorodoi deformation density (VDD) suggested recently.[53] An assesment of the Mulliken, Bader, Hirshfeld, Weinhold, and Voronoi Deformation Density (VDD) methods for charge analysis reported very recently is very informative.[53]

Within the BO approximation the electric dipole moment μ is calculated according to

$$\mu = e \sum_{A=1}^{M} Z_A \mathbf{R}_A - e \int \psi_i \sum_{i=1}^{N} \mathbf{r}_i \psi_i \, \mathrm{d}\tau$$

$$= e \sum_{A=1}^{M} Z_A \mathbf{R}_A - e \int P_i(\mathbf{r}) \, \mathbf{r} \mathrm{d}\tau$$

The first and second terms of the above equation represent the nuclear and electronic contributions to the dipole moment of the molecule, respectively.

Multiple moments (quadrupole, octapole, exapole and dodecapole) can also be calculated by computational quantum chemical techniques and the entire set of the electric moments is required to completely and exactly describe the distribution of charge in a molecule.

Electrostatic Potentials

The molecular electrostatic potential (MEP) is the energy, which a positive charge (an "electrophile") "feels" at any location in a molecule. The MEP is defined according to

$$MEP = \sum_{A=1}^{M} \frac{Z_A}{|\mathbf{r} - \mathbf{R}_A|} - \int \frac{\mathrm{d}\mathbf{r}' \rho(\mathbf{r})}{|\mathbf{r}' - \mathbf{r}|}$$

where the first and second terms represent the nuclear and electronic contributions to MEP, respectively.

The electrostatic potential is a physical property of a molecule related to how a molecule is first "seen" or "felt" by another approaching species, thereby has proven to be particularly useful in rationalizing the interactions between molecules and molecular recognition processes. This is because electrostatic forces are primarily responsible for long-range interactions between molecules. The electrostatic potential varies through space, and it can be visualized in the same way as the electron density. A portion of a molecule that has a negative electrostatic potential surface will be susceptible to electrophilic attack – the more negative the better. As non-covalent interactions between molecules often occur at separations where the van der Waals radii of the atoms are just touching, it is often most useful to examine the MEP in this region. For this reason, the MEP is often calculated at the molecular surface and is visualized from "color mapping" the value of the electrostatic potential onto an electron density surface, which corresponds to a conventional space-filling model. The resulting model simultaneously displays molecular size and shape and electrostatic potential value.

Vibrational Frequencies

Frequency runs are performed for two reasons either to actually predict the frequencies and the IR and Raman intensities or to confirm whether a stationary point found corresponds to a local (or global) minimum or to a saddle point. The calculation of the vibrational frequencies offers several advantages. First, the calculation leads not only to the position of the peaks, but also to the exact vibrational motion (normal vibrational mode) of the molecule to which the peak corresponds. Programs that offer graphical display of these motions are widely available, thus adding further in the visualization and understanding the origin of the effect we often see in the laboratory.

It should be noted that most quantum chemical studies of vibrational frequencies are carried out within the "double" harmonic approximation (i.e., using only second derivatives for the force constants and the derivative of the dipole moment for the intensities). Because calculations produce harmonic vibrational frequencies that do not include anharmonic effects—the so-called mechanical and electrical anharmonicities—we must be careful when comparing experimental and theoretical results.

As computational results of vibrational frequencies at various levels of theory have systematic errors, one can scale the computed values by an empirical factor characteristic for each level of theory.[54,55]

NMR Chemical Shifts

Nuclear magnetic resonance spectra (NMR) can also be computed using *ab initio* and density functional theories. However, the main problem in all calculations of magnetic properties (i.e., NMR chemical shifts and magnetizabilities) using finite basis sets is the gauge-invariance problem. This simply means that the results depend on the chosen gauge-origin, e.g., the chosen origin of the coordinate system (e.g., the calculated NMR chemical shifts will change if the molecule is "translated" along an axis). This clearly unphysical behavior can be avoided by assigning a local gauge-origin to each basis function, which is known as "gauge-including atomic orbitals" (GIAO).[56–60] Other approaches to the gauge-origin problem are the IGLO (individual gauge for localized orbitals) method of Kutzeling and Schinler,[61] the LORG (local orbitals-local origins) method of Hansen and Bouman,[62] and the CSGT (continuous set of gauge transformations) method.[63–65] The GIAO approach is the most elegant solution to the gauge-invariance problem and, in contrast to the IGLO method, is easily extended to correlated approaches.

The final results of an NMR calculation at any level of theory are the corresponding absolute isotropic magnetic shielding tensor elements, σ^{iso} (in ppm) as well as the anisotropic shielding, σ^{aniso} (in ppm) of all nuclei in the molecule. In order to compare with experimental results, one needs to carry out equivalent NMR calculation on the reference compound used and take the difference between the two calculations.

$$\delta = \sigma_{ref} - \sigma$$

With respect to basis sets, the following recommendation can be made. In the case of ^{11}B and ^{13}C nuclei a basis set of DZ quality is in most cases sufficient for relative shifts. Larger basis sets (i.e., TZ or even QZ) are in most cases not needed for the accurate prediction of chemical shifts. On the other side, ^{15}N, ^{17}O, and ^{19}F NMR chemical shift calculations require larger basis sets of at least TZ plus polarization quality (TZP). For other nuclei, not very much can be said at the moment and the user is strongly urged to check carefully the basis set dependence to ensure reliable theoretical results. However, limited experience suggests

that for second-row elements quite large basis sets are needed for accurate calculations.

In recent years the viability of DFT methods to the prediction of metal and ligand NMR shielding parameters in transition metal complexes has been highlighted in a steadily increasing number of studies and is now summarized in a series of recent review articles.[2c,66–68] The nuclear magnetic shielding tensor elements of a number of transition metal complexes ($[Co(CN)_6]^{3-}$, $[Co(NH_3)_6]^{3+}$, $Cr(CO)_6$, $[CrO_4]^{2-}$, $Fe(CO)_5$, $Fe(C_5H_5)_2$, $[MnO_4]^-$, $[Mn(CO)_6]^+$, $VOCl_3$, VF_5) were successfully predicted by DFT calculations within the LORG framework.[66] Moreover, the *ab initio*/GIAO methodology has been successfully applied to the theoretical calculation of complexation-induced chemical shifts ($\Delta\delta$) of zinc, ruthenium, rhodium and tin-porphyrin complexes, where the ^1H NMR resonance signals experience large ring-current-induced upfield shifts.[70]

Ionization Energies and Electron Affinities

According to Koopman's theorem the energy of an electron in an orbital is often equated with the energy required to remove the electron to give the corresponding ion. In this respect, the energy of the HOMO is interpreted as the negative of an ionization potential, I_p, while that of the LUMO as the negative of electron affinity, E_a:

$$\varepsilon_{HOMO} = -I_p$$
$$\varepsilon_{LUMO} = -E_a$$

However, when applying Koopman's theorem, two important caveats must be remembered. The first of these is that the orbitals in the ionized state M^+, are assumed to be the same as in the state, M; they are frozen. In other words the MOs for M^+ are not allowed to change (i.e., there is no relaxation). The second caveat is that there is no difference in the correlation energies of M and M^+. Correlation effects will tend to increase the ionization potential, while admitting orbital relaxation will tend to diminish the ionization potential. In many cases these two factors fortuitously cancel for valence electrons, with Koopman's theorem offering a reasonably good measure of the actual I_p.

For a molecule, if the energy difference is computed at the geometry of M, we obtain the so-called *vertical* ionization potentials (VIP). However, if we allow M^+ to relax to its optimum geometry before evaluating its energy, we get *adiabatic* ionization potentials (AIP). Obviously, the I_p

and E_a computed in the framework of Koopman's theorem are also vertical.

Considering that the number of electrons change during the ionization process, correlation effects are of particular importance for a proper description of the electron detachment processes. Therefore, highly correlated methods, such as CCSD(T) or modern DFT methods combined with a relatively large basis set, should be applied for the calculation of adiabatic I_p and E_a. In particular, for E_a diffuse functions should be added to the basis set to describe properly the anion M^-. For the $M+e \rightarrow M^-$ process there are actually three different quantities that can be computed: the vertical electron detachment energy (VEDE, energy to eject electron at the geometry of the anion); the adiabatic electron affinity (AEA, when the neutral M is allowed to relax to its optimum geometry) and the vertical electron affinity (VEA, where the geometry of the neutral is assumed for the anion).

Ionization potentials, electron affinities, and proton affinities are reproduced fairly well within gradient corrected DFT. However, more reliable results are obtained via propagator methods, such as the Outer Valence Green's Function (OVGF) method.[71]

Time-dependent Calculations

Time-dependent response theory (TDRT) is a powerful tool for the computation of electronic transitions (electronic spectra) and dynamic polarizabilities and hyperpolarizabilities.

Electronic spectra are more difficult to model. The problem originates from the fact that to obtain the electron density and energy in all *ab initio* calculations, the energy is minimized with respect to the density. If an excited-state energy and density are sought in this manner, there must be something in the theory to prevent the solution from collapsing to the ground state. A reliable quantum chemical treatment of electronic excitation in atoms and molecules requires in general a proper inclusion of static and dynamic effects of electron correlation. This makes it necessary to carry out extended multi-reference CI (MR-CI) calculations or complete active space plus perturbation theory in second order CAS-PT2 to reach an accuracy of about 0.1 eV in excitation energies.

To study the electronic spectra of transition metal coordination compounds, four types of quantum chemical computational techniques can be applied: (i) the variational SCF, CI and MCSCF approaches; (ii) the

time–dependent density functional theory (TD-DFT) approaches;[72–74] (iii) the coupled cluster approaches, such as the equation of motion CCSD (EOM-CCSD);[75] (iv) the single state (SS) or multistate (MS) second order perturbational approaches, such as the SS-CASP2 and MS-CASP2.[76] These methods are present in most of the quantum program packages available. An excellent review of the recent applications of quantum chemical computational techniques in the electronic spectroscopy and photoreactivity of transition metal coordination compounds by Daniel [2d] is very informative.

A single excitation interaction (CIS) calculation[77] is the most common procedure to get excited state energies. This has the advantage of being easier to use, but can only be used to treat excited states that are largely single excitations. A CIS calculation is not extremely accurate. However, it has the advantage of being able to compute many excited state energies easily. An essential feature of these calculations is that they report oscillator strengths for the transitions predicted. This is to help in comparing to actual spectra, since there are many excited states that can be calculated for a molecule but that have zero or near-zero intensities and therefore are not observed in the normal optical experiment.

INORGANIC CHEMISTRY BY ELECTRONIC STRUCTURE CALCULATION METHODS

In the past few years, several excellent reviews have appeared that describe the application of electronic structure calculation methods to a variety of difficult problems encountered in transition metal chemistry.[1–7] Therefore, here we will focus on a few selected case applications of electronic structure calculation methods to transition metal and organometallic chemistry, aiming to stimulate the interest of inorganic chemists willing to learn new science and to adapt to a somewhat different style than he or she is accustomed to, welcoming a combination of theory, computation, and experiment toward solution of difficult chemical problems of their interest. Such a synergistic process allows an "evolution" of solutions that can progressively address more of the complexity of the realistic problem and incorporate new physical data as they become available.

Exploring Bonding and Nonbonding Intermetallic M···M Interactions

Many important classes of transition metal coordination compounds and metalloenzymes exhibit bonding and nonbonding intermetallic

interactions. A detailed understanding of the nature of these interactions is of particular importance to understand the structure and reactivity of these molecular systems. The structural variability in dimetal systems that contain the simple ''diamond-shaped'' $M_2(\mu\text{-}X)_2$ core structure has attracted considerable interest from both the experimental and theoretical point of view. Of particular interest is a new class of bis(μ-oxo) dicopper and diiron systems comprising iron and copper centers in non-heme, multimetal enzymes, such as monooxygenases, fatty acid desaturase, and tyrosinase, which function in the activation of dioxygen to catalyze a diverse array of organic transformations. Aspects of the chemistry of copper and iron compounds containing the $M_2(\mu\text{-}O)_2$ core have been recently reviewed.[78]

The structural behavior of the $M_2(\mu\text{-}X)_2$ core has been analyzed theoretically by Alvarez[79] and Mealli.[80] Following the arguments of Alvarez the formation or breaking of trans-annular bonds in these systems is related to the number of framework electrons, e.g., the number of electrons involved in bonding between the metals and the bridging ligands. It was found that the allocation of the M-M based valence electrons into molecular orbitals of σ, π, δ, δ^*, π^*, and σ^* symmetries provides a wealth of information regarding the chemistry that these systems will posses.

A number of theoretical studies have led to a detailed picture of the bonding within the $Cu_2(\mu\text{-}O)_2$ core. The diamagnetic nature of complexes involving this core is consistent with the d^8 electronic configuration of Cu(III) and the tetragonal nature of the coordination sphere. The d^8-d^8 [LCu(III)(μ-O)$_2$Cu(III)L]$^{2+}$ (where L is a tridentate ligand) compounds having two bridging bonds, and a sufficient number of electrons to fill up all six σ, σ^*, π, π^*, δ, and δ^* Cu$\cdots$Cu orbitals do not involve intermetallic Cu$\cdots$Cu bonds.
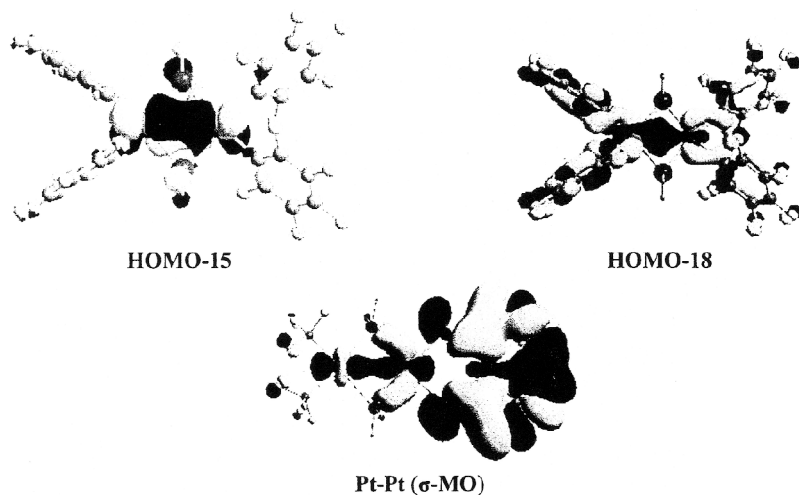
A similar bonding pattern has been established through quantum chemical calculations at the DFT level of theory, for an important class of phosphido-bridged μ-PR$_2$ compounds exhibiting a variety of M$\cdots$M$'$ (M = M$'$ = Pt or Pd; M = Pt, M$'$ = Pd) interactions.[81,82] The ability of such DFT methods (B3LYP functional, LANL2DZ, 6-31G basis set) to reproduce experimental geometry and identify the M$\cdots$M$'$ bonding interactions and its variation on oxidation in this class of complexes was demonstrated.

The d^8-d^8 phosphido-bridged diplatinum [(C$_6$F$_5$)$_2$Pt(μ-PPh$_2$)$_2$-Pt[(C$_6$F$_5$)$_2$]$^{2-}$ and trinuclear [(C$_6$F$_5$)$_2$M(μ-PPh$_2$)$_2$M$'$(μ-PPh$_2$)$_2$M$''$-(C$_6$F$_5$)$_2$]$^{2-}$ (M, M$'$, M$''$ = Pd(II), Pt(II)) compounds having sufficient

number of electrons to fill up all six MOs do not exhibit any intermetallic $M \cdots M'$ interaction. The calculations[81,82] indicated that oxidation of these complexes should be occur on the metal centers, since the highest occupied orbitals are mainly metal-based orbitals that are close in energy. In the oxidized d^7-d^7 phosphido-bridged $[(C_6F_5)_2Pt(\mu\text{-}PPh_2)_2\text{-}Pt[(C_6F_5)_2]$ and $[(C_6F_5)_2M(\mu\text{-}PPh_2)_2M'(\mu\text{-}PPh_2)_2M''(C_6F_5)_2]$ species having only ten electrons to occupy the six MM' orbitals, two bridging bonds resulting in a formal single Pt-Pt bond. The MOs contributing to the formation of the Pt(III)-Pt(III) bond in the oxidized species are depicted schematically in Scheme 1.
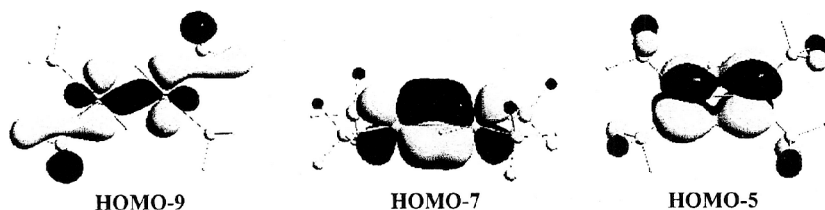
When the bridging ligand is hydride, as in the case of the catalytically active d^8-$d^8$$[(R_3Si)(PCy_3)Pt(\mu\text{-}H)_2Pt(R_3Si)(PCy_3)]$ hydrido-bridged diplatinum compound, the Pt-Pt interaction acquires a triple bond character (there are σ, π and δ MOs). This is substantiated by the respective molecular orbital interactions (Scheme 2), which correspond to σ-(HOMO-9), π-(HOMO-7) and δ- (HOMO-5) bonding interactions.

DFT calculations at the B3LYP/LANL2DZ level successfully reproduced the geometrical parameters of the hydrido-bridged diplatinum complexes (Figure 3) providing for the first time the position of the bridging hydride ligands, which otherwise could not be located by the X-ray

HOMO-15   HOMO-18

Pt-Pt (σ-MO)

Scheme 1. The MOs contributing to the formation of the Pt(III)$-$Pt(III) bonds in $[(C_6F_5)_2Pt(\mu\text{-}PH_2)_2Pt[(C_6F_5)_2]$ and $[(CF_3)_2Pt(\mu\text{-}PH_2)_2Pt(\mu\text{-}PH_2)_2Pt(CF_3)_2]$ complexes.
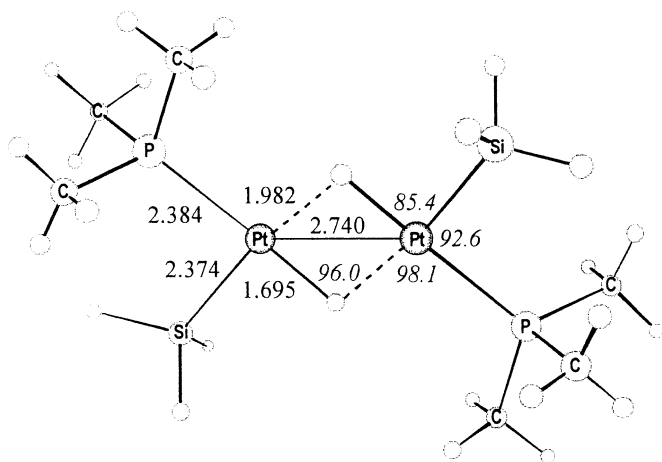
HOMO-9   HOMO-7   HOMO-5

Scheme 2. The most relevant molecular orbital interactions describing the Pt–Pt interactions in the model complex [(H$_3$Si)(PH$_3$)Pt(μ-H)$_2$Pt(H$_3$Si)(PH$_3$)].

crystallographic study.[83] The optimized geometries are of C_{2h} symmetry involving asymmetric Pt(μ-H)$_2$Pt bridges; the Pt-H and H$\cdots$Pt bond distances differ by about 0.3 Å.

Employing gradient-corrected levels of DFT ^{1}H, ^{31}P, ^{28}Si and ^{195}Pt chemical shifts were calculated at the GIAO B3LYP/LANL2DZ level of theory using the B3LYP/LANL2DZ equilibrium geometries. The chemical shift of the bridging hydride ligands was predicted to occur around 13.5 ppm, as expected for the resonances attributable to a platinum hydride found typically in the range τ^{13-27} ppm. The reliability of the computed ^{1}H *NMR* chemical shifts were assessed by the calculation of the ^{1}H *NMR* chemical shifts of complex [Pt$_2$(H)$_2$(μ-H)(μ-dpm)$_2$]$^+$

Figure 3. Equilibrium geometry of a model complex [{Pt(SiH$_3$)(μ-H)(PMe$_3$)}$_2$] computed at the B3LYP/LANL2DZ level of theory.

(dpm $= H_2PCH_2PH_2$), involving both symmetrical bridging and terminal hydride ligands at the same level of theory. It was found that the bridging hydride resonances are at τ 15.7 ppm, a value very close to the experimental one of τ 15.85 ppm of the "real" $[Pt_2(H)_2(\mu\text{-}H)(\mu\text{-}dppm)_2]^+$ (dppm $= Ph_2PCH_2PPh_2$) complex.[84]

The single two-electron reduction for the Fe-Fe bonded dinuclear complexes $Fe_2(CO)_6(\mu_2\text{-}PR_2)_2$ (R = Me or CF_3) with the "diamond-shaped" $Fe_2(\mu\text{-}PR_2)_2$ core structure was studied by DFT methods.[85] These complexes, being also d^7-d^7 phosphido bridged dimetal complexes, upon reduction undergo the simple structural change related to the cleavage of the intermetallic Fe-Fe bond. The experimentally observed cleavage of the Fe-Fe bond upon addition of electrons was reproduced in all calculations. This is because the added electrons occupy the LUMO of the complexes, which are Fe-Fe σ-antibonding. It was found that inclusion of solvation and/or ion pair effects in the computational model is crucia1 to correctly reproduce the experimentally observed energetic profile that favors the disproportionation reaction of the singly reduced complexes. The model that includes both a countercation and solvation is energetically and chemically the most realistic model. Moreover, the self-consistent reaction field (SCRF) method to treat solvation effects, such as COSMO, was found to be well suited for modeling the changes in electronic structure arising from solvation.

Ab initio calculations at the HF level using relatively small basis sets and ECPs for Pt, P and Cl atoms have been carried out for a series of model Pt(II) dimmers with bridging S^{2-} and RS^- ligands, involving the $Pt_2(\mu_2\text{-}S)_2$ core, in order to elucidate the determinants of the structure, planar or hinged.[86] It was found that electronic rather than steric effects govern the geometry of the $Pt_2(\mu_2\text{-}S)_2$ core; the decrease of the through-ring antibonding interaction between the in-plane sulfur p orbitals with folding appears to be the determinant for hinging.

DFT calculations at the B3LYP/SDD level of theory also threw light on the bonding mechanism in a series of halo-bridged Cu(I) dimers, with a diamond like structure of D_{2h} symmetry.[87] It was predicted that the Cu-X bond involves both σ- and π-dative bonding components. Most important is the presence of π-type MOs delocalized over the entire four-membered $Cu(\mu\text{-}X)_2Cu$ ring, which supports a ring current and could probably account for the nearly equivalent Cu-X bonds in the rhombus. Moreover, all $[Cu(\mu\text{-}X)(PH_3)_2]_2$ dimers exhibit a σ-type MO corresponding to weak Cu$\cdots$Cu interactions supporting through-ring
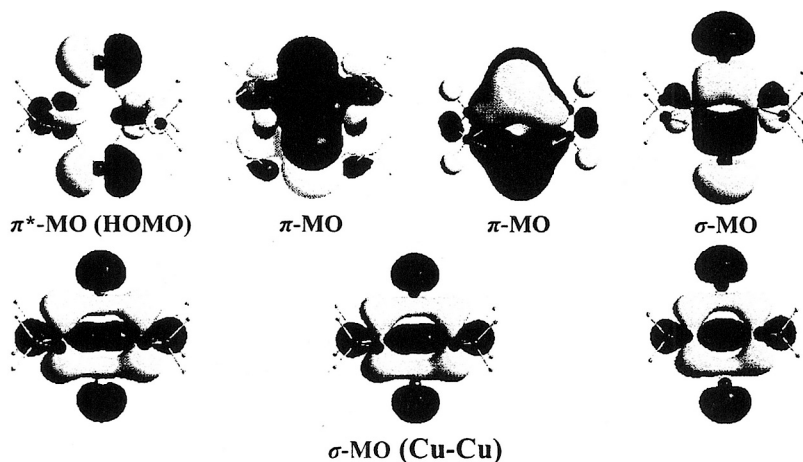
intermetallic interactions, which seems to be responsible for the stabilization of the otherwise unstable anti-aromatic $Cu(\mu\text{-}X)_2Cu$ ring (the metallacycle ring having a total of 8 framework electrons does not conform to the Hückel rule of aromaticity). The intermetallic Cu···Cu distance is tuned by the identity of the halide ligand, X, following paradoxically the trend:

$Cu(\mu\text{-}I)Cu < Cu(\mu\text{-}Br)Cu < Cu(\mu\text{-}Cl)Cu$.

The shortest Cu···Cu distance was observed for the best electron-donating bridged iodide ligand. An electron density topological analysis assigned a bond order for the Cu···Cu interaction in the chloro-derivative of 0.2, which increases to 0.6 in the hydrido bridged dimmer with a much shorter Cu···Cu separation distance. All halo-bridged copper(I) dimers exhibit a similar pattern of molecular orbital level diagram with a successive lowering of the respective eigenvalues ongoing from the chloro- to iodo-derivatives. This is consistent with the higher stability of the iodo complex in the series. The most important molecular orbitals of the halo-bridged copper dimmers are collected in Scheme 3.

The nature of the very short bond (around 260 pm) between platinum and thallium in the experimentally known $[(NC)_5Pt\text{-}Tl(CN)n]^{n-}$ (n = 0−3) compound has been investigated[88] by electronic structure calculation methods at RHF, DFT and MP2 levels using model compounds $[H_5Pt\text{-}TlH_n]^{n-}$. The simplest picture of the short Pt-Tl bonds corresponds to an approximate $\sigma^2\pi^4$ triple bond comprising two parts, σ donation from Tl to the empty coordination site of L_5Pt^- and π donation from the off-axis Pt-L bonds to the $6p\pi$ orbital of Tl. This bonding character is consistent with the observed oxidation states between $Pt^{IV}\text{-}Tl^{1}$ and $Pt^{II}\text{-}Tl^{III}$. Moreover, relativistic DFT study of $[(NC)_5Pt\text{-}Tl(CN)]^-$ demonstrated that the remarkable experimentally observed spin-spin coupling pattern, e.g., $^2J(Tl\text{-}C) \gg {}^1J(Tl\text{-}C)$ and $J(Pt\text{-}Tl) \sim 57\,kHz$, is semiquantitatively reproduced if both relativistic effects and solvation are taken into account. Solvent effects are very substantial and shift the Pt-Tl coupling by more than 100%, e.g. Relativistic increase of s-orbital density at the heavy nuclei, charge donation by the solvent, and the specific features of the multicenter C-Pt-Tl-C bond are responsible for the observed coupling pattern.[89]

The mechanism of "metallophilic" interactions, e.g. the attractions between formally closed shell metal d^{10} centers (archetypically a pair of

π*-MO (HOMO) π-MO π-MO σ-MO

σ-MO (Cu-Cu)

Scheme 3. The most important molecular orbitals of the halo-bridged copper(I) dimmers.

Au(I) cations) has been exhaustively investigated by Pyykkö and cowor-
kers using the HF and MP2 *ab initio* methods. The theoretical treatment
of these strong closed-shell interactions in inorganic chemistry has also
been reviewed by Pyykkö.[90] Energy partitioning schemes have been used
to investigate the metallophilic attraction between Au(I), Ag(I) and Cu(I)
centers in model dimmers of $[X\text{-}M\text{-}PH_3]_2$ (X = H, Cl) type.[91] The main
part of the attraction involves pair correlation between one $M(d^{10})$ entity
and non-$M(d^{10})$ localized orbitals of the partner monomer. It was also
predicted that at r_e(M-M) dispersive and non-dispersive components
are about equally important for all systems considered. The contribution,
due to nd-nd interaction, falls drastically along the series Au > Ag > Cu.

The aurophilicity phenomenon has been the subject of many theoreti-
cal treatments. From these studies, it was concluded that aurophilicity is a
genuine correlation-dispersion effect, enhanced by induction and, in parti-
cular, by relativistic corrections, which may all be quite strong in heavy
atomic systems. The coexistence of Au(I)-Au(I) contacts and hydrogen
bonding in the model systems $[H_2P(OH)AuCl]_2$ and $[H_2P(OH)AuH_2(O)]_2$
studied at the MP2 level illustrated that the two interactions are compara-
ble.[92] The aurophilic interactions between gold atoms in the different oxi-
dation states Au(I)-Au(I), Au(I)-Au(III) and Au(III)-Au(III) have also
been investigated at the MP2 level of theory and the dispersion, induction
and electrostatic multipole components to the aurophilic attraction were
analyzed using intermolecular models.[93]

More recently[94] the electronic and geometric structures of Cl-M-PH$_3$ and [Cl-M-PH$_3$]$_2$ (M = Cu, Ag, Au) have been studied computationally using post-HF *ab initio* and DFT methods. Including electron correlation through the QCISD, CCSD and CCSD(T) calculations changes the trend in metallophilic interaction; the interaction decreases along the series Ag → Au → [111]. Moreover, the overall performance of different quantum chemical approaches (HF, MP2 and five different DFT methods) concerning the Au-Au distances and bond dissociation energies for fifteen molecules containing the Au(I) species has very recently been investigated by Wang and Schwarz.[95] It was found that simple density functionals (LDF) of the Slater (or Slater plus Vosko) type yield rather reasonable results, while common gradient corrected DF are not recommended, nor are the large core pseudopotentials for Au. As far as the aurophilic bonding mechanism is concerned both one-electron (i.e., electrostatic, polarization, charge transfer, and orbital interactions) and two-electron effects (i.e., correlation, dispersion) contribute significantly to the Au(I)-Au(I) interactions.

Finally, heteronuclear metal-metal contacts between gold(I) and group -11, -12 and -13 elements have been investigated both experimentally and theoretically and their chemistry has been reviewed by Laguna and Bardaji.[96] The metallophilic interactions, in these gold-metal contacts are predicted to be of intermediate strength relative to the homonuclear metal-metal interactions. In general, metallophilic interactions are found in bridged or unbridged pairs, oligomers, chains, and sheets involving, among others, main-group elements (such as Se and Te), d^{10} ions [such as Cu(I), Ag(I) and Au(I)], s^2 ions [such as Tl(I) and In(I)], and also d^8 ions [such as Ir(I)]. A recent survey of such interactions by Grader[97] is very informative. Of particular importance are the extremely strong $6s^2$-$6s^2$ intermetallic interactions in [AuBa]$^-$ and [AuHg]$^-$ diatomics studied recently by Wesendrup and Schwerdtfeger.[98]

EXPLORING THE MECHANISM OF CATALYTIC GAS-PHASE REACTIONS INVOLVING TRANSITION METALS

In recent years gas phase reactions between transition metal atoms or ions and the inherently stable thermodynamically small molecules, such as CO_2, CH_4, NH_3, H_2O and H_2 have attracted considerable interest.[5,99–113] This interest is primarily due to the fact that these reactions may serve as models for understanding the reactivity pattern of
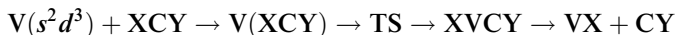
transition–metal–based catalysts in condensed phase. Moreover, the complexes formed may serve as potential precursors for the challenging task of activation of these molecules and provide simple model systems to probe fundamental bonding interactions.[114] Transition metal ions are particularly suitable for this purpose because of their rich gas phase chemistry.[115] Only a few representative examples of catalytic gas phase reactions involving transition metals will be discussed herein, for the inorganic chemist to get insight how electronic structure calculation methods helps in understanding the corresponding reaction mechanisms.

The coordination of carbon dioxide to first transition row metal cations and the insertion reaction of the metal into one $C=O$ bond of carbon dioxide have been studied theoretically at the B3LYP level.[110b] Binding energies have also been determined at the CCSD(T) level using large basis sets. The most favorable coordination of CO_2 is the linear end-on M^+-**O**CO one, due to the electrostatic nature of the bonding. The ground state and binding energies are mainly determined by several mechanisms for reducing metal-ligand repulsion. For the early transition metals (Sc^+, Ti^+, and V^+), the insertion reaction is exothermic and the OM^+CO structure is more stable than the linear M^+-**O**CO isomer, because of the very strong MO^+ bond that is formed. More recently,[110c] the electronic and geometrical structures of $3d$-metal neutral, MCO, anionic $[MCO]^-$, and cationic $[MCO]^+$ monocarbonyls, (M = Sc to Cu), were computed using DFT with generalized gradient approximation for the exchange-correlation potential. The calculated adiabatic electron affinities and ionization potentials are in good agreement with experiment. The reaction $[MCO]^{0,-,+} + CO \rightarrow [MC]^{0,-,+} + CO_2$ was found to be significantly less endothermic than the 130.3 kcal/mol found for gas phase CO. Among the neutrals, this reaction is endothermic by 30.0 kcal/mol for Mn, while Fe is found to be the second best atom, with the reaction being endothermic by 36.7 kcal/mol.

The gas-phase reaction of the nickel atom with CO_2 molecule was investigated at the B3LYP and CCSD(T) levels of theory.[109c] The lowest energy path proceeds through the $^3A''$ ONiCO intermediate and yields the $^3\sum^-$ NiO and CO. An electron transfer from the Ni atom to the CO_2 molecule initiates the metal insertion reaction and then the insertion and oxygen-abstraction steps take place in a concerted fashion along with the charge-transfer processes. The insertion reaction is direct and needs to overcome an energy barrier of 34.6 kcal/mol. The $Ni + CO_2 \rightarrow$

NiO + CO reaction was found to be endothermic by 37.4 kcal/mol, in good agreement with experiment (36.6 kcal/mol).

The reactions of the ground-state $V(s^2d^3)$ atoms with the isovalent CO_2, CS_2, and OCS molecules have been studied at the B3LYP level.[108a] The comparative study of the reactions:

$$V(s^2d^3) + XCY \rightarrow V(XCY) \rightarrow TS \rightarrow XVCY \rightarrow VX + CY$$

with XCY = CO_2, CS_2, and OCS showed that insertion reaction proceeds on a single potential energy surface ($^4A''$) along one intrinsic reaction co-ordinate, the CX (X = O,S) bond length. Comparison of relative energies illustrated that insertion products are always more stable than the related coordination species, with the following increasing orders of stability: $V(OCS) < V(CO_2)$, $V(CS_2)$ and OVCS < OVCO < SVCS, SVCO. Only the $V + CO_2 \rightarrow VO + CO$ and $V + OCS \rightarrow VS + CO$ reactions are exo-thermic, with a low or no activation barrier for the insertion reaction.

The $^2A'$ and $^2A''$ potential energy surfaces, for the $Sc + CO_2 \rightarrow ScO + CO$ reaction were explored by B3LYP and CCSD(T) methods independently by Papai et al.[109b] and by Hwang and Mebel[108] in order to gain insight into the mechanism of the reaction. Both $^2A'$ and $^2A''$ state $Sc + CO_2$ reactions lead to spontaneous metal insertion into CO_2. How-ever, only the $^2A'$ state insertion complex can readily dissociate, into ScO + CO. The entrance channel of the reaction corresponds to the η^2-**C,O** coordination of the CO_2 molecule.

Very recently[111b] the mechanism of the CO_2-to-CO reduction by ground-state Fe atoms has been investigated in the framework of elec-tronic structure calculations at the B3LYP level of theory, using the 6-31G(d) and 6-311+G(3df) basis sets. The $Fe + CO_2 \rightarrow FeO + CO$ reaction predicted to be endothermic by 23.24 kcal/mol could follow two possible alternative pathways depending on the nature of the entrance channel involving formation of either a $Fe(\eta^2$-**OCO**) or a $Fe(\eta^3$-**OCO**) intermedi-ate. The $Fe(\eta^2$-**OCO**) intermediate was found to be weakly bound with respect to $Fe(^5D)$ and CO_2 dissociation products, but strongly bound relative to the separated $Fe^+(^6D)$ and $[CO_2]^-$ anion; the computed Fe-CO_2 bond dissociation energy is predicted to be 207.3 kcal/mol. On the other hand, the $Fe(\eta^3$-**OCO**) intermediate is unbound with respect to $Fe(^5D)$ and CO_2 dissociation products by 8.3 kcal/mol, but also strongly bound relative to the separated $Fe^+(^6D)$ and $[CO_2]^-$ anion; the computed Fe-CO_2 bond dissociation energy is predicted to be 198.3 kcal/ mol. Both reaction pathways involve an intramolecular insertion reaction

of the Fe atom into the O-C bond of the $Fe(\eta^2\text{-}\mathbf{OCO})$ or $Fe(\eta^3\text{-}\mathbf{OCO})$ intermediates yielding the isomeric $OFe(\eta^1\text{-}\mathbf{CO})$ or $OFe(\eta^1\text{-}\mathbf{OC})$ insertion products, respectively with a relatively low activation barrier.

The mechanism of the reaction $YS^+ + CO_2 \rightarrow YO^+ + COS$ in the gas phase has been studied at the B3LYP level of theory by Xie.[112] The reaction proceeds via two four-center transition states with a cyclic intermediate complex. The reaction mechanism includes seven stationary points (reactants, three intermediate complexes, two transition states TS and products) on the reaction potential surface. The activation barriers of the two transition states are -8.3 and $2.1\,\text{kcal/mol}$, respectively, indicating that the second reaction step should be the rate-determining reaction step.

The catalytic activity of bare cationic transition metal monoxides (MO^+) towards methane is a key to the mechanistic aspects in the direct methane hydroxylation. The reaction pathway and energetics for methane-to-methanol conversion by first row transition metal oxide cations has thoroughly been investigated by Yoshizawa et al.[106] using the B3LYP density functional approach. Both high-spin and low-spin PESs were characterized at the B3LYP/6-311G(d,p) level of theory. The methane activation process proceeds via two transition states following the course: $MO^+ + CH_4 \rightarrow OM^+(CH_4) \rightarrow [TSl] \rightarrow HO\text{–}M^+\text{-}CH_3 \rightarrow [TS2] \rightarrow M^+(CH_3OH) \rightarrow M^+ + CH_3OH$ (M = Sc, Ti, V, Cr, Mn, Fe, Co, Ni, and Cu). A crossing between high-spin and low-spin PESs occurs once near the exit channel for ScO^+, TiO^+, VO^+, CrO^+, and MnO^+, but it occurs twice in the entrance and exit channels for FeO^+, CoO^+, and NiO^+. In most cases the high-spin and low-spin PESs have crossing points, in the vicinity of which spin inversion can take place. This nonadiabatic electronic process is a manifestation of the so-called *two-state reactivity* (TSR) concept, which is of particular interest in organometallic chemistry and oxidation catalysis.[99f] The TRS phenomenon involving participation of spin inversion in the rate-determining step can dramatically affect reaction mechanisms, rate constants, branching ratios, and temperature behaviors of organometallic transformations. Some recent case studies involving TRS, namely the $V^+ + CS_2$ system, the hydroxylation of methane by FeO^+ and the β-Hydrogen transfer in $[FeC_5H_5]^+$ cation are presented and discussed in ref. 99f.

Density functional B3LYP and CCSD(T) calculations have also been employed to investigate potential energy surfaces for the reactions of neutral scandium, nickel, and palladium oxides with methane. The results

show that NiO and PdO are reactive toward methane and can form molecular complexes with CH_4 bound by 9–10 kcal/mo1 without a barrier. At elevated temperatures, the dominant reaction channel is direct abstraction of a hydrogen atom by the oxides from CH_4 with a barrier of about 16 kcal/mol leading to MOH (M = Ni, Pd) and free methyl radical. On the other hand, scandium oxide is not reactive with respect to methane at low and ambient temperatures. At elevated temperatures (when a barrier of about 22 kcal/mol can be overcome), the reaction can produce the CH_3ScOH molecule, but the latter is not likely to decompose to the methyl radical and ScOH or Sc + CH_3OH because of the high endothermicity of these processes.[108b] The minimal energy reaction pathway for methane conversion to methanol using nickel and palladium oxides involves both triplet and singlet PESs, which is another example of the TRS concept. The same holds true for the insertion reaction of Zn, Cd, and Hg atoms with methane and silane studied at the BPW91 density functional and MP2 levels of theory.[116]

The TSR paradigm is also characteristic for the dehydrogenation reactions of H_2O, NH_3, and CH_4 molecules by $Mn^+(^7S, {}^5S)$ and Fe^+ (^6D, ^4F) cations investigated at the B3LYP level using a DZVP basis set optimized ad hoc for the employed functional [113]. In all cases, the low-spin ion-dipole complex, which is the most stable species on the respective PESs, is initially formed. In the second step, a hydrogen shift process leads to the formation of the insertion products, which are more stable in a low-spin state. The low- and high-spin PESs have crossing points, in correspondence of which spin inversion takes place. The topological analysis of the *electron localization function* (ELF) has been used to characterize the nature of the bonds for all of the minima and transition states along the paths. Depending on the presence of lone pairs in the ligand, two different bonding mechanisms have been identified. This has been achieved by analyzing DFT calculations (B3LYP approach) using the bonding evolution theory. The different domains of structural stability occurring along the reaction path have been identified as well as the bifurcation catastrophes responsible for the changes m the topology of the systems. The analysis provides a chemical description of the reaction mechanism in terms of agostic bond formation and breaking. After the formation of the first reaction intermediate, all the three reactions are equivalent from a bonding evolution viewpoint, since the presence of a trisynaptic basin, which corresponds to the condensation of two covalent bonds into a three-center bond, is verified in all the three cases.

The reactions of first row transition metal cations with water have also been investigated in detail.[100] Both the low- and high-spin PESs have been characterized at the B3LYP/DZVP level of theory. Energy differences between key low-and high-spin species and total reaction energies for the possible products have been predicted at even higher levels of theory. The expected trend for the $M(OH_2)^+$ ion-molecule dissociation energies has been well described through the row. Whereas the only exothermic products of the $M^+ + H_2O$ reaction for M = Sc to V were $MO^+ + H_2$ with exothermicity decreasing from Sc to V, the afore-mentioned reactions were endothermic for M = Cr to Cu with endo-thermicity increasing through the series. As in the $Fe^+ + H_2O$ system, less difference between the high- and low-spin structures was observed for the late transition metals than in the early transition metal systems. The reason for this is that the high-spin Fe^+ to Cu^+ cations have at least one set of paired electrons while the Sc^+ to Mn^+ high-spin cations do not. Both high- and low-spin PESs cross once in the entrance channel for Sc^+ to Mn^+. Two crossings were observed, at the entrance and exit channels, on the Fe^+ PESs. Finally, the surfaces of Co^+ to Cu^+ demonstrate one crossing near the exit channel.

The mechanism of H_2 oxidation by FeO^+ has been investigated by density functional calculations using the B3LYP, BP86, and FT97 functionals and an extended basis set.[105b] Three mechanisms were considered, addition-elimination, "rebound," and oxene-insertion. The addition-elimination and "rebound" mechanisms are competitive, exhibiting TRS with a crossing between sextet and quartet states. TSR provides a low-energy path for bond activation and is predicted to be the dominant pathway at room temperature. Both TSR mechanisms are concerted: the addition-elimination mechanism involves $2 + 2$ addition in the bond activation step, while the rebound mechanism is effectively concerted, involving the H-abstraction followed by a barrierless "rebound" of the H-radical.

Finally, the interaction of first row transition metal dications (Mn^{2+} to Cu^{2+}) with a single water molecule has been studied at the B3LYP and CCSD(T) level of theory using triple-zeta basis sets.[107] The results obtained provided strong evidence for the possibility to observe the $[M(OH_2)]^{2+}$ complexes as long-lived species in the gas phase with abun-dance increasing toward the left-hand in the Periodic Table. In particular, for $[Cu(OH_2)]^{2+}$ and $[Cu(OH_2)_2]^{2+}$ complexes, although the dissociation products $Cu^+ + H_2O^+$ from $[Cu(OH_2)]^{2+}$ are lower in energy than

$Cu^{2+} + H_2O$, an avoided crossing of the $Cu^{2+} \cdots OH_2$ and $Cu^+ \cdots OH_2^+$ PESs provides a minimum in the adiabatic PES, which predicts that $[Cu(OH_2)]^{2+}$ should be a stable gas phase ion. The activation barrier for the decomposition of $[Cu(OH_2)]^{2+}$ to $Cu^+ + H_2O^+$ is about 27 kJ/mol, whereas the barrier height, for the decomposition of $[Cu(OH_2)_2]^{2+}$ to $[Cu(OH_2)]^+ + H_2O^+$ is much larger (167 kJ/mol). Based on these results, El-Nahas et al.[117] predicted the existence of $[Cu(OH_2)_2]^{2+}$ in the gas phase, under suitable conditions, and probably the much less stable $[Cu(OH_2)]^{2+}$. Actually, recent experimental results [118] vindicated the theoretical predictions that the cupric ion solvated by one and two water molecules should be stable species and therefore exist in the gas phase.

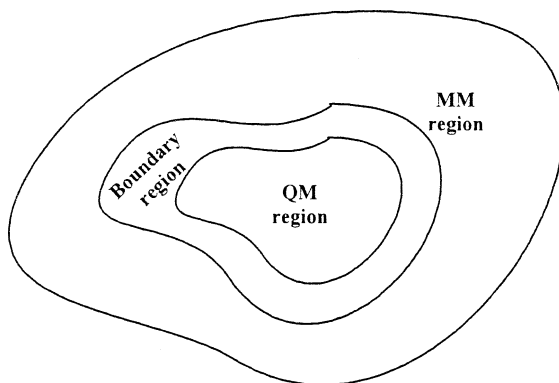## EXPLORING THE CATALYTIC CYCLE OF SYNTHESIS REACTIONS CATALYZED BY TRANSITION METAL-CONTAINING CATALYSTS

In the last few years, several excellent reviews have appeared that describe the application of electronic structure calculation methods to reactions of transition metal compounds. Niu and Hall[1a] have reviewed the theoretical studies on reactions of transition metal complexes, while Frenking et al.[1d] gave an extensive overview of theoretical studies of some transition metal mediated reactions of industrial and synthetic importance. In a more recent review, Harvey et al.[2n] surveyed a number of recent studies concerning spin-forbidden reactions that occur in coordination chemistry. These reactions concern ligand dissociation/association, oxidative addition and migratory insertion reactions, which play an important role in homogeneous catalytic processes. For spin-forbidden reactions the *minimum energy crossing points* (MECPs) between states of different spin can be located for large, realistic transition–metal–containing systems yielding important new insight into their mechanism. Moreover, recent books have also been devoted to computational organometallic chemistry[119] and the theoretical aspects of homogeneous catalysis.[120]

It is our wish to comment here on the more recent developments in the area, presenting a few case examples of homogeneous catalytic processes investigated by electronic structure calculation methods. In general terms, computational modelling of catalytic processes requires a high-level quantum chemical treatment. However, the down side is that quantum chemical methods require tremendous computational resources.

Due to the expense of quantum chemical calculations, the detailed study of a catalytic cycle often involves a stripped–down model of the chemical system. This methodology is followed when we want to treat relatively big-sized molecular systems at a high level of theory. The use of models resulting upon substitution of peripheral components by simpler substituents and removing the solvent molecules does not alter the description of the "core" region of the compounds and is ultimately the most efficient and productive route to modelling the electronic structure and related properties of relatively big-sized transition metal coordination compounds. It should be emphasized that great care has to be exercised in choosing the simpler substituents. These substituents might exhibit similar electronic properties with those they are going to substitute. This is because in some cases the peripheral components act only as spectators, but in others, they can substantially influence the PES. Thus, quantum chemical models that neglect the surrounding molecular environment might lead to limited or even erroneous conclusions. Another popular approach to simulate complex molecular systems, such as the transition metal catalyzed synthesis or enzyme reactions at the quantum chemical level, is the combined quantum mechanics and molecular mechanics (QM/MM) method.[121–123] In this hybrid method, part of the molecular potential, such as the catalyst's or metalloenzyme's active site, is determined by QM calculation, while the remainder of the molecular potential is determined using a much faster molecular mechanics (MM) calculation. The QM/MM method's promise is that it allows for simulation of bond breaking and formation at the active site, while still taking into account the role of the extended system in an efficient and computationally tractable manner.

The QM/MM method's key feature is that a QM calculation is performed on a truncated QM model of the active site with the large ligands removed and replaced by capping atoms. Then, a MM calculation is performed on the remainder of the system. The division of the full system into two sub-systems (Scheme 4) may require cutting a covalent bond. Different techniques have been developed to treat this problem, fulfilling the valence of the quantum atom placed in the boundary with hydrogen atoms or frozen orbitals.

The QM (e.g. reacting) region "feels" the influence of the molecular mechanics environment—for example, the atomic charges of the MM atoms affect the QM atoms. By combining the accuracy of a QM method (for a small reacting system) with the speed of a MM method (for its

Scheme 4. Schematic representation of the setup of a QM/MM calculation. A small region containing the reacting atoms is treated by a quantum mechanical method (e.g. molecular orbital theory), and its surroundings are represented more simply by molecular mechanics.

surroundings), reactions in large molecules and in solution can be studied. In this way the wave function of the quantum subsystem, and thus any related property, can be obtained under the influence of the environment. In the QM/MM method, the molecular system is described by a mixed Hamiltonian:

$$H = H_{QM} + H_{MM} + H_{QM/MM}$$

and the total energy of the system can be written as:

$$E = E(QM) + E(QM/MM) + E(MM) + E(boundary)$$

The energy of the QM system, $E(QM)$, and the energy of the MM system, E(MM), are calculated exactly as they would be in a standard calculation at those levels. $E(QM/MM)$ is the interaction energy between the QM and MM regions (e.g. due to the interaction of the MM atomic charges with the QM system), while E(boundary) is the energy due to any boundary restraints applied to the outer edge of the MM region to maintain its structure.

A characteristic example of the successful application of the hybrid QM/MM method for a more realistic computational simulation of complex systems concerns the Brookhart-type Ni-diimine and group-4 diamide olefin polymerization catalysts.[124] The structure of the "real" system and the corresponding model QM system for which the electronic structure calculation is performed are shown in Figure 4. The hydrogen
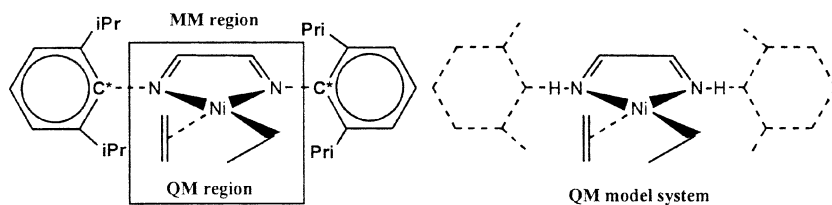
Figure 4. An example of QM/MM partitioning in a Ni-diimine olefin polymerization catalyst.

atoms cap the electronic system and are termed "dummy" atoms. The dummy atoms correspond to "link" atoms in the real system, that are labeled C.

More recently, Tobisch and Ziegler reported on a comprehensive theoretical investigation of the influence of ligand L on the regulation of the selectivity for the [Ni^{0}L]-catalyzed cyclodimerization of 1,3-butadiene based on DFT and a combined DFT/MM (QM/MM) method.[125] The role of electronic and steric effects has been elucidated for all crucial elementary steps of the entire catalytic cycle. Moreover, both the thermodynamic and the kinetic aspects of the regulation of the product selectivity have been fully understood.

DFT has also been used to study the reaction mechanism and structure-reactivity relationships in the stereospecific 1,4-polymerization of butadiene catalyzed by neutral allylnickel(II) halide [Ni(C$_3$H$_5$)X]$_2$ (X$^-$ = Cl$^-$, Bi$^-$, I$^-$) complexes[126] using stripped–down models of the catalytic system for the computational effort to be kept moderate. All crucial steps of the catalytic cycle, such as monomer π complex formation, symmetrical and unsymmetrical splitting of dimeric π complexes, and *anti-syn* isomerization, have been scrutinized.

The *regio-* and *stereo-*selectivity in palladium-catalyzed electrophilic substitution of aryl chlorides with aromatic and heteroaromatic aldehydes has recently been studied at the B3PW91/DZ + P level of theory.[127] The two most important factors controlling the selectivity were found to be the location of the phenyl functionality in the η^1-moiety of the bis(allyl)palladium intermediate and the relative configuration of the phenyl substituents in the cyclic six-membered transition state of the reaction.

A few theoretical studies[128–132] have recently been devoted to the study of olefin metathesis reactions catalyzed by the Grubbs-type

ruthenium carbene $[(PR_3)(L)Cl_2Ru=CH_2]$ (L=PR$_3$ or imidazol-2-ylidene, NHC) complexes[128]. Both the associative and dissociative mechanism of olefin metathesis reaction catalyzed by the model $[(PH_3)(L)Cl_2Ru=CH_2]$ (L=PH$_3$ or NHC) complexes have thoroughly been investigated by Thiel and coworkers[129] using DFT techniques with the BP86 and B3LYP functionals. These functionals combined with medium-size basis sets provided realistic geometries, relative energies and vibrational frequencies. Moreover, for further validation, additional CCSD(T) calculations were performed on the BP86 geometries. The dissociative mechanism with olefin coordination in a *trans*-position with respect to the ancillary ligand, L is favored over all other alternatives. The π-bonded olefin and the metallacycle species were identified as intermediates, while the rate-determining step was found to be the ring closure-opening processes of these species in terms of the calculated ΔG^0_{298} values. However, the calculated ΔH^0_{298} values for phosphine dissociation from the "precatalyst" are in opposite trend with experimental results, but conforming to the strength of the *trans* influence of the ancillary ligand, L. At the same time Cavalo[130] reported a DFT study of the first generation "real" Grubbs-type catalysts $[(PCy_3)(Cl)_2(L)Ru=CHPh]$ with L=PCy$_3$ or NHC along with some of the Hofmann's[131] cationic Ru-based catalysts with chelating bisphospine ligands following a dissociative mechanism with *trans*-olefin coordination to the "active" catalyst. The author found that the binding energy of PCy$_3$ ligand to the Ru central atom of the "precatalyst" is larger when the *trans* ancillary ligand L is NHC rather than PCy$_3$. These results are in line with the experimental data reported by Grubbs as well as with the DFT results reported by Hermann and coworkers.[131] More recently, Botoni *et al.*[132] investigated the mechanism of the metathesis reaction catalysed by Grubbs-type catalysts at the B3LYP level of theory using the DZVP basis set. Among the three different paths considered for olefin metathesis reaction with the model catalysts $[Cl_2(L)_2Ru=CH_2]$ (L=PH$_3$ or PPh$_3$) the following two seem to be the most probable: the mechanism conforming to the proposed mechanism by Grubbs [128] and the mechanism supporting the results reported by Hofmann *et al.*[131]

Most recently, the important synthesis reaction the copper-catalyzed cyclopropanation reaction has been studied theoretically.[133–135] Bühl *et al.*[133] performed DFT calculations at the BP86/AEl level of theory with augmented Wachters' basis on Cu and 6-31G(d) basis on all other elements using model catalytic systems. For the big-sized models the

Stuttgart-Dresden (SDD) relativistic effective core potentials have been used. The calculations illustrated that the mechanism of the Cu-catalyzed olefin cyclopropanation involves, as key intermediates, Cu(carbene) species that have been confirmed either free or in the form of complexes with the reactant olefin.

The exploration of the PES of a medium-size reaction model of copper-catalyzed cyclopropanation reactions at the B3LYP/6-31l+ G(2d,p)//B3LYP/6-31G(d) level of DFT by Garcia *et al.* [134] elucidated the key steps of the catalytic cycle. It was found that the cyclopropanation step takes place through a direct carbene insertion of the copper-carbene species to yield a catalyst-product complex, which can finally regenerate the starting complex. In a more recent paper[135] the authors investigated the role of a counterion in Cu-catalyzed enentioselective cyclopropanation reactions at the same level of theory using medium-sized reaction models. The presence of a coordinated counteranion was found to affect significantly the geometries of the reaction intermediates and transition structures, but not the overall reaction mechanism or the key reaction pathway. The rate-determining step was found to be the nitrogen extraction from a catalyst-diazoester complex to generate a copper-carbene intermediate.

The mechanism of the copper-catalyzed cyclopropanation reaction has also been studied by Rasmussen *et al.*[136] at various levels of density functional and *ab initio* theory using a variety of basis sets. The calculations were performed on small model systems using quantum chemical computational techniques of high level or on "real" systems using the hybrid QM/MM computational approach. Solvation corrections were evaluated by using B3LYP/LACVP together with the BP-SCRF solvation model. The selectivity-determining step in the copper-catalyzed cyclopropanation proceeds by a concerted but very asynchronous addition of a metallacarbene to the alkene. Ligand-substrate interactions influencing the enantio- and diastereo-selectivity have been identified, and the preferred orientation of the alkene substrate during the addition is suggested.

SUMMARY AND OUTLOOK

In this work, we have provided a guided tour of the use of quantum chemical computational techniques in solving problems that inorganic chemists face, enabling them to acquire enough information to form a good concept of what the work is about. Theoretical studies have

significantly improved our understanding of the metal-ligand bonding modes and throw light onto the details of the inorganic reaction mechanisms for a number of industrially and synthetically important reactions. The recent advances in the field of quantum inorganic chemistry hold great promise for the future discovery of new series of novel transition metal coordination compounds with particular properties and functionality, guiding experimentalists to synthesize them. A general recipe for a successful application of computational quantum chemistry is as follows:

(i) Choose the appropriate computational method. DFT is the widely accepted computational technique for transition metal coordination chemistry.

(ii) Choose with care the basis set of the highest possible quality for the system of interest. For heavy metals use relativistic ECPs, such as LANL2DZ or SDD, while for the rest of the atoms use at least the 6-31 G(d) basis set. For anionic species diffuse functions must be added as well.

(iii) Perform single point calculations at a higher level of theory, such as CCSD(T) with a larger basis set, on the optimized geometry, when it is computationally possible with the computational resources available to get more realistic energetic data.

(iv) Construct with care a model with computationally convenient size to represent the "real" big-sized systems or use the hybrid QM/MM method. By combining the accuracy of a QM method (for a small reacting system) with the speed of an MM method (for its surroundings), reactions in large molecules and in solution can be studied.

(v) Include solvation in studies of reaction mechanisms involving charged species to correctly predict the energetic reaction profile.

(vi) Determine the structures and energies of reactants, transition states, intermediates and products when reaction mechanisms are studied.

(vii) Investigate the factors controlling the reactivity and selectivity of the particular reaction and create rules for the design of new compounds.

(viii) Compute spectra, such as IR, NMR, Raman, UV-Vis, PES, etc., which can help in identifying new compounds and predict their reactivity.

(ix) Apply charge density and energy partitioning schemes to get insight into the bonding mechanism and the reactivity of the molecular system of interest.

In spite of the progress carried out in the field of quantum inorganic chemistry, a long path is still waiting to be walked. The scope of applications of electronic structure calculation methods is still far from mature. We have to look for new methodological developments, as well as for more careful assessment of applicability. There is an ongoing effort to improve DFT methods through a systematic improvement of the functionals based on a pure theoretical basis aiming to find the exact functional. Ultimately, highly parallel machines may very well be the most effective way to solve many of the computational bottlenecks. Combining large number of powerful computers, as long as an efficient parallel algorithm, can extend some of the higher-level electronic structure calculation methods into the metaloenzyme and metal cluster regime. A daunting challenge for the future is to accurately model chemical reactions in phases and at the active site of metalloenzymes. An ability to do so would be of great importance in designing new biological catalysts as well as fully understanding the chemical mechanism of those that already exist. This would be of significant technological as well as scientific importance. One could imagine that many new molecules could be made and made much more efficiently by such catalysts. Recently, there is much interest in using DFT for predicting the correct spin ground state of high spin species very abundant in the realm of inorganic chemistry. Moreover, the scope of applications of DFT grows rapidly with calculations of new molecular properties being added to actively developed software. Finally, effective core potential methods coupled with parallel supercomputing are expected to constitute an exciting approach towards the goal of developing methods for addressing the chemistry of all heavy elements of the Periodic Table.

REFERENCES

1. (a) Niu, S., and M. B. Hall 2000. *Chem. Rev.*, 100, 353; (b) Loew, G. H., and D. L. Harris, 2000. *Chem. Rev.*, 100, 407; (c) Siegbahn, P. E. M., and M. R. A. Blomberg, 2000. *Chem. Rev.*, 100, **421**; (d) Torrent, M., M. Solà, and G. Frenking, 2000. *Chem. Rev.*, 100, 439; (e) Rohmer, M.-M., M. Bènard, and J.-M. Poblet, 2000. *Chem. Rev.*, 100, 495; (f) Dedieu, A., 2000. *Chem.*

Rev., 100, 543; (g) Maseras, A., A. Lledós, E. Clot, and O. Eisenstein 2000. *Chem. Rev.*, 100, 601; (h) Alonso, J. A., 2000. *Chem. Rev.*, 100, 637; (i) Harrison, J. F., 2000. *Chem. Rev.*, 100, 679; (k) Frenking, G., and N. Fröhlich, 2000. *Chem. Rev.*, 100, 717; (l) Hush, N. S., and J. R. Reimers, 2000. *Chem. Rev.*, 100, 775; (m) Ceulemans, A., L. F. Chibotaru, G. A. Heylen, K. Pierloot, and L. G. Vanquickenborne, 2000. *Chem Rev.*, 100, 787; (n) Cundari, T. R., 2000. *Chem. Rev.*, 100, 807.

2. (a) Comba, P., and R. Remaenyi, 2003. *Coord. Chem. Rev.*, 238–239, 9; (b) Ellis, D. E., and O. Warschkow, 2003. *Coord. Chem. Rev.*, 238–239, 31; (c) Autschback, J., and T. Ziegler, 2003. *Coord. Chem. Rev.*, 238–239, 83; (d) Daniel, C., 2003. *Coord. Chem. Rev.*, 238–239, 143; (e) Newton, M. D., 2003. *Coord. Chem. Rev.*, 238–239, 167; (f) Ciofini, L., and C. A. Daul, 2003. *Coord. Chem. Rev.*, 238–239, 187; (g) Lovell, T., F Himo, W.-G. Han, and L. Noodleman, 2003. *Coord. Chem. Rev.*, 238–239, 211; (h) Erras-Hanauer, H., T. Clark, and R. van Eldik, 2003. *Coord. Chem. Rev.*, 238–239, 233; (i) Georgakaki, I. P., L. M. Thomson, E. J. Lyon, M. B. Hall, and M. Y. Darensbourg, 2003. *Coord. Chem. Rev.*, 238–239, 255; (j) Friesner, R. A., M.-H. Baik, B. F. Gherman, V. Guallar, M. Wirstam, R. B. Murphy, and S. J. Lippard, 2003. *Coord. Chem. Rev.*, 238–239, 267; (k) Boone, A. J., C. H. Chang, S. N. Greene, T. Herz, and N. G. J. Richards, 2003. *Coord. Chem. Rev.*, 238–239, 291; (l) Webster, C., and M. B. Hall, 2003. *Coord. Chem. Rev.*, 238–239, 315; (m) Renhold, J., A. Barthel, and C. Mealli, 2003. *Coord. Chem. Rev.*, 238–239, 333; (n) Harvey, J. N., R. Poli, and K. M. Smith, 2003. *Coord. Chem. Rev.*, 238–239, 347; (o) Sapunov, V. N., R. Schmid, K. Kirchner, and H. Nagashima, 2003. *Coord. Chem. Rev.*, 238–239, 363; (p) Macchi, P., and A. Sironi, 2003. *Coord. Chem. Rev.*, 238–239, 383.

3. Tsipis, C. A., 1991. *Coord. Chem. Rev.*, 108, 163.

4. Koga, K., and K. Morokuma, 1991. *Chem. Rev.*, 91, 823.

5. Gordon, M. S., and T. R. Cundari, 1996. *Coord. Chem. Rev.*, 147, 87.

6. Noodleman, L., T. Lovell, W.-G. Han, J. Li and F. Himo, 2004. *Chem. Rev.*, 104, 459.

7. Solomon, E. I., R. K. Szilagyi, S. DeBeer George, and L. Basumallick, 2004. *Chem. Rev.*, 104, 419.

8. http://www.chem.swin.edu.au/chem ref.html#Software.

9. http://cmm.info.nih.gov/modeling/universal_software.html.

10. Cramer, C. J., 2002. *Essentials of Computational Chemistry*, Wiley, Chichester.

11. Feller, D., E. R. Davidson, in: Lipkowitz, K. B., and D. B. Boyd (Eds.), 1990. *Reviews in Computational Chemistry*, vol. 1, VCH, New York.

12. Krishnan, R., M. J. Frisch, and J. A. Pople, 1980. *J. Chem. Phys.*, 72, 4244.

13. Wilson, A. K., T. van Mounk, and T. H. Dunning, 1996. *J. Mol. Struct.*, 388, 339.

14. Hay, P. J., 1977. *J. Chem. Phys.*, 66, 4377.

15. Stevens, W. J., M. Krauss, H. Basch, and P. G. Jasien, 1992. *Can. J. Chem.*, 70, 612.

16. Frenking, G., I. Antes, M. Bohme, S. Dapprich, A. W. Ehlers, V. Jonas, A. Neuhaus, M. Otto, R. Stegmann, A. Veldkamp, and S. F. Vyboischclukov, in: Lipkowitz, K. B., and D. B. Boyd (Eds.), 1996. Reviews in *Computational Chemistry*, vol. 8, VCH, New York.

17. Schmidt, M. W., and M. S. Gordon, 1998. *Annu. Rev. Phys. Chem.*, 49, 233.

18. Gilson, H. S. R., and M. Krauss, 1998. *J. Phys. Chem.*, A, 102, 6525.

19. Roos, B. O., K. Anderson, M. P. Fülscher, P. A. Malmqyist, L. Serrano-Andres, K. Pierloot, M. Merchan, 1996. *Adv. Chem. Phys.*, 93, 219.

20. Palmer, I. J., I. N. Ragazos, F. Bernardi, M. Olivucci, and M. A. Robb, 1993. *J. Am. Chem. Soc.*, 115, 673.

21. Olivucci, M., I. N. Ragazos, F. Bernardi, and M. A. Robb, 1993. *J. Am. Chem. Soc.*, 115, 3710.

22. Barlett, R. J., and J. F. Stanton, in: Lipkowitz, K. B., and D. B. Boyd (Eds.), 1994. *Reviews in Computational Chemistry*, vol. 5, p. 65, VCH, New York.

23. Møller, C., and M. S. Plesset, 1934. *Phys. Rev.*, 46, 618.

24. Čížek, J., 1966. *J. Chem. Phys.*, 45, 4526.

25. Čížek, J., 1969. *Adv. Chem. Phys.*, 14, 35.

26. Čížek, J., and J. Paldus, 1971. *Int. J. Quantum. Chem.*, 5, 359.

27. Pople, J. A., D. P. Santry, and G. A. Segal, 1965. *J. Chem. Phys.*, 43, 129.

28. (a) Dewar, M. J. S., and W. Thiel, 1977. *J. Am. Chem. Soc.*, 99, 4899; (b) Thiel, W., in: Schleyer, P. V. R., N. L. Allinger, T. Clark, J. Gasteiger, P. A. Kollman, H. F. Schaefer, III, and P. R. Schreiner (eds.), 1998. *Encyclopedia of Computational Chemistry*, vol. 3, Wiley, Chichester, p. 1599.

29. (a) Dewar, M. J. S., E. G. Zoebisch, E. F. Healy, and J. P. Stewart, 1985. *J. Am. Chem. Soc.*, 107, 3902; (b) Holder, A. J., in: Schleyer, P. V. R., N. L. Allinger, T. Clark, J. Gasteiger, P. A. Kollman, H. F. Schaefer, III, and P. R. Schreiner (eds.), 1998. *Encyclopedia of Computational Chemistry*, vol. 1, Wiley, Chichester, p. 8.

30. (a) Stewart, J. J. P., 1989. *J. Comput. Chem.*, 10, 209; (b) Stewart, J. J. P., in: Schleyer, P. V. R., N. L. Allinger, T. Clark, J. Gasteiger, P. A. Kollman, H. F. Schaefer, III, and P. R. Schreiner (eds.), 1998. *Encyclopedia of Computational Chemistry*, vol. 3, Wiley, Chichester, p. 2080.

31. Hehre, W. J., and J. Yu, Book of Abstracts, 210th ACS National Meeting, Chicago, IL, 20/24 August, 1995 (Pt. 1).

32. http://www.chachesoftware.co./mopac/index.shtml.

33. Koch, W., and M. C. Holthausen, 2000. *A Chemist's Guide to Density Functional Theory*, Wiley-VCH, Weinheim.

34. Bartolotti, L. J., and K. Flurchick, in: K.B. Lipkowitz, D.B. Boyd (Eds.), 1996. *Reviews in Computational Chemistry*, vol. 7, VCH, New York.

35. Parr, R. G., and W. Yang, 1989. *Density-Functional Theory of Atoms and Molecules*, Oxford University Press, Oxford.

36. Ellis, D. E., 1995. *Density Functional Theory of Molecules, Clusters, and Solids*, Kluwer Academic Publishers, Dordrecht.

37. Geerlings, P., F. De Proft, and W. Langenaeker, 2003. *Chem. Rev.* 103, 1793.

38. Vosko, S. H., L. Wilk, and M. Nusair, 1980. *Can. J. Phys.* 58, 1200.

39. Perdew, J. P., and Y. Wang, 1992. *Phys. Rev.* B 45, 13244.

40. Perdew, J. P., and Y. Wang, 1986. *Phys. Rev.* B 33, 8800.

41. Perdew, J. P., 1986. *Phys. Rev.* B 33, 8822.

42. (a) Becke, A. D., 1993. *J. Chem. Phys.*, 98, 5648; (b) Becke, A. D., 1988. *Phys. Rev.* B 38, 3098; (c) Lee, C., W. Yang, and R. G. Parr, 1998. *Phys. Rev.* B 37, 785; (d) Curtiss, L. A., K. Raghavachari, P. C. Redfern, J. A. Pople, 1997. *J. Chem. Phys.* 106, 1063.

43. (a) Lynch, B. J., P. L. Fast, M. Harris, and D. G. Truhlar, 2000. *J. Phys. Chem. A*, 104, 4811; (b) Lynch, B. J. and D. G. Truhlar, 2001. *J. Phys. Chem. A*, 105, 2936.

44. Shadhukhan, S., D. Munoz, C. Adamo, and G. E. Scuseria, 1999. *Chem. Phys. Lett.* 306, 83.

45. Pavese, M., S. Chawla, D. Lu, J. Lobaugh, and G. A. Voth, 1997. *J. Chem. Phys.* 107, 7428.

46. Schlegel, H. B., 2003. *J. Comput. Chem.* 24, 1514.

47. (a) Mulliken, R. S., 1995. *J. Chem. Phys.*, 23, 1833; (b) Mulliken, R. S., 1955. *J. Chem. Phys.*, 23, 1841; (c) Mulliken, R. S., 1955. *J. Chem. Phys.*, 23, 2338; (d) Mulliken, R. S., 1955, *J. Chem. Phys.*, 23, 2343.

48. (a) Reed, A. F., R. B. Weinstock, and F. A. Weinhold, 1985. *J. Chem. Phys.*, 83, 735; (b) Reed, A. F., L. A. Curtiss, and F. A. Weinhold, 1988, *Chem. Rev.*, 83, 899.

49. Bader, R. F. W., 1990. *Atoms in Molecules. A Quantum Theory.* Clarendon Press, Oxford, UK.

50. Hirshfeld, F. L., 1977. *Theoret. Chim. Acta*, 44, 129.

51. (a) Politzer, P., and R. R. Harris, 1970. *J. Am. Chem. Soc.*, 92, 6451; (b) Politzer, P., and E. W. Stout, Jr., 1971. *Chem. Phys. Lett.*, 8, 519; (c) Politzer, P., 1971. *Theoret. Chim. Acta*, 23, 203.

52. Rousseau, B., A. Peeters, and C. Van Alsenoy, 2001. *J. Mol. Struct.*, 538, 235.

53. Fonseca, C., G. J.-W. Handgraaf, E. J. Baerends, and F. M. Bickelhaupt, 2004. *J. Comput. Chem.*, 25, 189.

54. Scott, A. P., and L. Radom, 1996. *J. Phys. Chem.*, 100, 16502.

55. Halls, M. D., J. Velkovski, and H. B. Schlegel, 2001. *Chem. Accounts*, 105, 413.

56. London, F., 1937. *J. Phys. Radium.*, 8, 397.

57. McWeeny, R., 1962. *Phys. Rev.*, 126, 1028.

58. Ditchfield, R., 1974. *Mol. Phys.*, 27, 789.

59. Dodds, J. L., R. McWeeny, and A. J. Sadlej, 1980. *Mol. Phys.*, 41, 1419.

60. Wolinski, K., J. F. Hilton, and P. Pulay, 1990. *J. Am. Chem. Soc.*, 112, 8251.

61. Kutzeinigg, W., 1980. *Isr. J. Chem.*, 19, 193.

62. Hansen, A. E., and T. D. Bouman, 1985. *J. Chem. Phys.*, 82, 5035.

63. Keith, T. A., and R. F. W. Bader, 1992. *Chem. Phys. Lett.* 194, 1.

64. Keith, T. A., and R. F. W. Bader, 1993. *Chem. Phys. Lett.* 210, 223.

65. Cheeseman, J. R., M. J. Frisch, G. W. Trucks, and T. A. Keith, 1996. *J. Chem. Phys.* 104, 5497.

66. Bühl, M., M. Kaupp, O. L. Malkina, V. G. Malkin, 1998. *J. Comput. Chem.*, 20, 91.

67. Schreckenbach, G., and T. Ziegler, 1998. *Theor. Chem. Accounts*, 99, 71.

68. Kaupp, M., O. L. Malkina, V. G. Malkin, P. Pyykkö, 1998. *Chem. Eur. J.*, 4, 118.

69. Wilson, P. J., R. D. Amos, and N. C. Handy, 2000. *Phys. Chem. Chem. Phys.*, 2, 187.

70. Gomila, R. M., D. Quinonero, C. Garau, A. Frontera, P. Ballester, A. Costa, and P. M. Deyà, 2002. *Chem. Phys. Lett.* 036, 72.

71. (a) Ortiz, J. V., 1988. *J. Chem. Phys.*, 89, 6348; (b) von Niessen, W., J. Schirmer, and L. S. Cederbaum, 1984. *Comp. Phys. Rep.* 1, 57; (c) Zakrzewski, V. G., and J. V. Ortiz, 1995. *Int. J. Quant. Chem.* 53, 583; (d) Ortiz, J. V. 1998. *Int. J. Quant. Chem. Symp.* 22, 431; (e) Ortiz, J. V. 1999. *Int. J. Quant. Chem. Symp.* 23, 321; (f) Ortiz, J. V., V. G. Zakrzewski, and O. Dolgounircheva, in: *Conceptual Perspectives in Quantum Chemistry*, 1997. Calais J.-L., and E. Kryachko (Eds.), Kluwer Academic, 465.

72. Jamorski, C., M. E. Casida, and D. R. Salahub, 1996. *J. Chem. Phys.*, 104, 5134.

73. Casida, M. E., 1996. *Recent Advances in Density Functional Methods*, World Scientific, Singapore.

74. Casida, M. E., 1996. in: J.M.S. Ed. (Editor), *Recent Developments and Applications of Modern DFT*, Elsevier Science, Amsterdam, pp. 391–434.

75. (a) Comeau, D. C., and R. J. Bartlett, 1993. *Chem. Phys. Lett.*, 207, 414; (b) Geertsen, J., M. Rittby, and R. J. Bartlett, 1989. *Chem. Phys. Lett.*, 164, 57; (c) Sekino, H., and R. J. Bartlett, 1984. *Int. J. Quantum Chem. Symp.*, 18, 225; (d) Stanton, J. F. and R. J. Bartlett, 1993. *J. Chem. Phys.*, 98, 7029; (e) Stanton, J. F., and R. J. Bartlett, 1993. *J. Chem. Phys.*, 98, 9335.

76. (a) Andersson, K., P.-A. Malmqvist, B. O. Roos, A. J. Sadlej, and K. Wolinski, 1990. *J. Phys. Chem.*, 94, 5483; (b) Andersson, K., P. A. Malmqvist, and B. O. Roos, 1992. *J. Chem. Phys.*, 96, 1218; (c) Andersson, K., B. O. Roos, P.-A. Malmqvist, and P.-O. Widmark, 1994.

Chem. Phys. Lett. 230, 391/434; (d) Finley, J., P.-A. Malmqvist, B. O. Roos, L. Serrano-Andrés, 1998. *Chem. Phys. Lett.*, 288, 299.

77. Foresman, J. B., M. Head-Gordon, J. A. Pople, and M. J. Frisch, 1992. *J. Phys. Chem.*, 96, 135.

78. Que, L. Jr., and W. B. Tolman, 2002. *Angew. Chem. Int. Ed.*, 41, 1114.

79. Alverez, S., A. A. Palacios, and G. Aullón, 1999. *Coord. Chem. Rev.*, 185–186, 431, and references cited therein.

80. (a) Mealli, C., and D. M. Proserpio, 1990. *J. Am. Chem. Soc.*, 112, 5484; (b) Mealli, C., and A. Orandini, 1999 in: *Metal Clusters in Chemistry*, Braunstein P., L. A. Oro, and P. R. Raithby, Wiley-VCH, Weinheim, vol. 1, p. 143–162.

81. Alonso, E., J. M. Casas, F. A. Cotton, X. Feng, J. Forniés, C. Fortuño, M. Tomás, 1999. *Inorg. Chem., 38*, 5034.

82. Alonso, E., J. M. Casas, J. Forniés, C. Fortuño, A. Martin, A. Guy Orpen, C. A. Tsipis, and A. C. Tsipis, 2001. *Organometallics 20*, 5571.

83. Tsipis, C. A., A. C. Tsipis, and C. E. Kefalidis, 2004. *Fundamental World of Quantum Chemistry*, vol. 3 Kluwer Academic Publishers, Dordrecht, The Netherlands.

84. Brown, M. P., R. J. Puddephatt, M. Rashidi, and K. R. Seddon, 1978. *J. Chem. Soc, Dalton, Trans.*, 516.

85. Baik, M.-H., T. Ziegler, and C. K. Schauer, 2000. *J. Am. Chem. Soc., 122*, 9143.

86. Captevila, M., W. Clegg, P. González-Duarte, A. Jarid, and A. Lledós, 1996. *Inorg. Chem.*, 35, 490.

87. Aslanidis, P., P. J. Cox, S. Divanidis, and A. C. Tsipis, 2002. *Inorg. Chem.*, 41, 6875.

88. Pyykkö, P., and M. Patzschke, 2003. *Faraday Discuss.*, 124, 41.

89. Autschbach, J., and T. Ziegler, 2001. *J. Am. Chem. Soc*, 123, 5320.

90. (a) Pyykkö, P., 1997. *Chem. Rev.*, 97, 597; (b) Pyykkö, P., and T. Tamm, 1998. *Organometallics*, 17, 4842.

91. Magnko, L., M. Schweizer, G. Rauhut, M. Schütz, H. Stoll and H.-J. Werner, 2000. *Phys. Chem. Chem. Phys.*, 4, 1006.

92. Mendizabal, F., P. Pyykkö and N. Runeberg, 2003. *Chem. Phys Lett.*, 370, 733.

93. Mendizabal, F., and P. Pyykkö, 2004. *Phys. Chem. Chem. Phys.*, 6, 900.

94. O'Grady, E., and N. Kaltsoyannis, 2004, *Phys. Chem. Chem. Phys.*, 6, 680.

95. Wang, S.-G., and W. H. E. Schwarz, 2004. *J. Am. Chem. Soc.*, 126, 1266.

96. Bardaji, M., and A. Laguna, 2003. *Eur. J. Inorg. Chem.*, 3069.

97. Gade, L. H., 2001. *Angew. Chem. Int. Ed.*, 40, 3573.

98. Wesendrup, P., and P. Schwerdtfeger, 2000. *Angew. Chem. Int. Ed.*, 907.

99. (a) Schröder, D., A. Fiedler, M. F. Ryan, and H. Schwarz, 1995. *J. Phys. Chem.*, 98, 1994; (b) Schröder, D., and H. Schwarz, 1995. *Angew. Chem.*

Int. Ed., 34, 1973; (c) Holthausen, M. C., A. Fiedler, H. Schwarz, and W. Koch, 1996. *J. Phys. Chem.*, 100, 6236; (d) Dieterle, M., J. N. Harvey, C. Heinemann, J. Schwarz, D. Schröder, and H. Schwarz, 1997. *Chem. Phys. Lett.*, 277, 399; (e) Bronstrup, M., D. Schröder, and H. Schwarz, 1999. *Chem. Eur. J.*, 5, 1176; (f) Schröder, D., and H. Schwarz, 2000. *Acc. Chem. Res.*, 33, 139.

100. (a) Irigoras, A. J. E. Fowler, and J. M. Ugalde, 1998. *J. Phys. Chem. A.*, 102, 293; (b) Irigoras, A. J. E. Fowler, and J. M. Ugalde, 1999. *J. Am. Chem. Soc.*, 121, 574; (c) Irigoras, A. J. E. Fowler, and J. M. Ugalde, 1999. *J. Am. Chem. Soc.*, 121, 8549; (d) Irigoras, A. J. E. Fowler, and J. M. Ugalde, 2000. *J. Am. Chem. Soc.*, 122, 114.

101. Clemmer, D. E., and P. B. Armentrout, 1994. *J. Phys. Chem.*, 98, 68.

102. Hall, C., and R. N. Perutz, 1996. *Chem. Rev.*, 96, 3125.

103. Nakao, Y., T. Taketsugu, and K. Hirao, 1999. *J. Chem. Phys.*, 110, 10863.

104. Kooi, S. E., and A. W. Castleman, 1999. *Chem. Phys. Lett.*, 315, 49.

105. (a) Danovich, D., and S. Shaik, 1997. *J. Am. Chem. Soc.*, 119, 1773; (b) Filatov, M., and S. Shaik, 1998. *J. Phys. Chem. A*, *102*, 3835.

106. (a) Yoshizawa, K., Y. Shiota, and T. Yamade, 1998. *J. Am. Chem. Soc.*, 120, 564; (a) Shiota, Y., and K. Y. Yoshizawa. 2000. *J. Am. Chem. Soc.*, 122, 12317.

107. El-Nahas, A. M., 2001. *Chem. Phys. Lett.*, 345, 325.

108. (a) Hwang, D.-Y., and A. M. Mebel, 2002. *Chem. Phys. Lett.*, 357, 51; (b) Hwang, D.-Y., and A. M. Mebel, 2002. *J. Phys. Chem. A.*, 106, 12072.

109. (a) Pápai, I., Y. Hannachi, S. Gwizdala, and J. Mascetti, 2002. *J. Phys. Chem. A.*, 106, 4181; (b) Pápai, I., G. Schubert, Y. Hannachi, and J. Mascetti, 2002. *J. Phys. Chem. A.*, 106, 9551; (c) Hannachi, Y., J. Mascetti, A. Stirling, and I. Pápai, 2003. *J. Phys. Chem. A.*, 107, 6708.

110. (a) Souter, P. F., and L. Andrews. 1997. *J. Am. Chem. Soc.*, 119, 7350; (b) Sodupe, M. V. Branchadell, M. Rosi, and C. W. Bauschlicher Jr. 1997. *J. Phys. Chem. A.*, 101, 7854; (c) Gutsev, G. L., L. Andrews and C. W. Bauschlicher Jr. 2003. *Chem. Phys.*, 290, 47.

111. (a) Karipidis, P., A. C. Tsipis, and C. A. Tsipis, 2003. *Collect. Czech. Chem. Comman.*, 68, 423; (b) Pantazis, D. A., A. C. Tsipis, and C. A. Tsipis, 2003. *Collect Czech. Chem. Commun.*, 69, 13.

112. Xie, X.-G., 2004. *Chem. Phys.*, 299, 33.

113. (a) Michelini, M. del C., E. Sicilia, N. Russo, M. E. Alikhani, and B. Silvi, 2003. *J. Phys. Chem. A, 107*, 4862; (b) Chiodo, S., O. Kondakova, M. del C. Michelini, N. Russo, E. Sicilia, A. Irigoras, and J. M. Ugalde, 2004. *J Phys. Chem. A*, *108*, 1069.

114. Dincan, M. A., 2000. *Int. J. Mass Spectrom.*, 200, 545, and references therein.

115. Freiser, B. S., 1996. *Organometallic Ion Chemistry*, Kluwer, Dordtrecht.

116. Alikhani, M. E., 1999. *Chem. Phys. Lett.*, 313, 608.

117. El-Nahas, A. M., N. Tajima, and K. Hirao, 2000. *Chem. Phys. Lett.*, 318, 333.

118. Stone, J. A., and D. Vukomanovich, 2001. *Chem. Phys. Lett.*, 346, 419.

119. Cundari, T. R., 2001. *Computational Organometallic Chemistry*, Marcel Decker, New York.

120. van Leeuwen, P. W. N. M., K. Morokuma, and J. H. van Lenthe, 1995. *Theoretical Aspects of Homogeneous Catalysis, Applications of ab initio Molecular Orbital Theory.* Kluwer Academic Publishers, Dordrecht, The Netherlands.

121. Field, M. J., P. A. Bash, and M. Karplus, 1990. *J. Comp. Chem.* 11, 700.

122. Maseras, F., and K. Morokuma, 1995. *J. Comp. Chem.* 16, 1170.

123. (a) Freindorf, M., and J. Gao, 1996. *J. Comp. Chem.* 17, 386; (b) Gao, J. 1996. *Acc. Chem. Res.* 29, 298; (c) Gao, J., 1996. *Reviews in Comp. Chem.*, 7, 119; (d) Gao, J., P. Amara, C. Alhambra, and M. J. Field, 1998. *J. Phys. Chem. A* 102, 4714; (e) Reuter, N., A. Dejaegere, B. Maigret, and M. Karplus, 2000. *J. Phys. Chem. A* 104 1720.

124. (a) Deng, L., T. K. Woo, L. Cavallo, P. M. Margl, and T. Ziegler, 1997. *J. Am. Chem. Soc.*, 119, 6177; (b) Deng, L., T. Ziegler, T. K. Woo, P. Margl, and L. Fan, 1998. *Organometallics*, 17, 3240: (c) Woo, T. K., P. M. Margl, L. Deng, L. Cavallo, and T. Ziegler, 1999. *Catalysis Today*, 50, 479; (d) Woo, T. K., S. Patchkovskii, and T. Ziegler, 2000. *Computing in Science and Engineering*, 28.

125. (a) Tobisch, S., and T. Ziegler, 2002. *J. Am. Chem. Soc.*, 124, 4881; (b) Tobisch, S., and T. Ziegler, 2002. *J. Am. Chem. Soc.*, 124, 13290.

126. Tobisch, S., and R. Taube, 2001. *Chem. Eur. J.*, 7, 3681.

127. Wallner, O. A., and K. J. Szabó, 2003. *Chem. Eur. J.*, 9, 4025.

128. (a) Sanford, M. S., M. Ulman, and R. H. Grubbs, 2001. *J. Am. Chem. Soc.*, 123, 749; (b) Sanford, M. S., J. A. Love, and R. H. Grubbs, 2001. *J. Am. Chem. Soc.*, 123, 6543.

129. Vyboishchikov, S. F., M. Bühl, and W. Thiel, 2002. *Chem. Eur. J.*, 8, 3962.

130. Cavallo, L., 2002. *J. Am. Chem. Soc.*, 124, 8965.

131. Weskamp, T. F. J. Kohl, W. Hieringer, D. Gleich, and W. A. Herrmann, *Angew. Chemie. Int. Ed.*, 1999, 38, 2416.

132. Bernardi, F., A. Botoni, and G. P. Miscione, 2003. *Organometallics*, 22, 940.

133. Bühl, M., F. Terstegen, F. Löffler, B. Meynhardt, S. Kierse, M. Müller, C. Näther, and U. Lüning, 2001. *Eur. J. Org. Chem.*, 2151.

134. Fraile, J. M., J. I. García, V. Martínez-Merino, J. A. Mayoral, and L. Salvatella, 2001. *J. Am. Chem. Soc.*, 123, 7616.

135. Fraile, J. M., J. I. García, M. J. Gil, V. Martínez-Merino, J. A. Mayoral, and L. Salvatella, 2004. *Chem. Eur. J.*, 10, 758.

136. Rasmussen, T., J. F. Jensen, N. Éstergaard, D. Tanner, T. Ziegler, and P.-O. Norrby, 2002. *Chem. Eur. J.*, 8, 177.